factors, IL-6 has drawn attention as a new therapeutic target. IL-6 blockade attenuates skin sclerosis induced by bleomycin in animal models (11), and tocilizumab, an anti–IL-6 receptor monoclonal antibody, improves dermal sclerosis in a subset of SSc patients (12). Supporting this notion, a recent study demonstrated the contribution to skin sclerosis of the Th17 subset, whose differentiation is regulated by IL-6 (13).

Previous studies have demonstrated the role of innate immunity in the pathogenesis of autoimmune diseases, including SSc (14). Innate immune response is mediated, in part, by Toll-like receptors (TLRs), which are evolutionarily conserved receptors for foreign pathogen-associated molecular patterns (15). TLRs and their ligands contribute to inflammatory responses, including autoimmune diseases, as well as host defenses by innate immunity (16), and they further control adaptive immune responses (17). Microbial TLR ligands trigger onset in experimental models of arthritis, diabetes, and atherosclerosis (18). Furthermore, various endogenous molecules serve as ligands for TLRs. TLR-4, originally identified as the receptor for lipopolysaccharide (LPS), recognizes hyaluronic acid (HA), fibronectin fragments, heparan sulfate, and high mobility group box 1 (HMGB-1) as endogenous ligands (18). This recognition is profoundly related to the persistent inflammatory and/or fibrotic process in collagen diseases (19).

In SSc patients, serum levels of HA and HMGB-1 and expression of HA in lesional skin are elevated (20–22). TLR-4 stimulation by these molecules results in fibroblast activation by augmenting transforming growth factor β (TGFβ) signaling (22). Importantly, in C3H/HeJ mice with point mutations in the *Tlr4* gene, bleomycin-induced skin sclerosis is attenuated despite the elevation of endogenous TLR-4 ligands (22). These results indicate that TLR-4 signaling activation is potentially involved in the fibrotic process of SSc and its animal models, at least partly by directly activating dermal fibroblasts. However, given that C3H/HeJ mice exhibit several defects, including spontaneous alopecia development caused by unknown immunologic abnormalities (23), the exact role of TLR-4 in the pathologic process of tissue fibrosis remains unknown. Therefore, we generated bleomycin-treated and tight skin mice with TLR-4 deletion and investigated the significance of TLR-4 in these models. Our results indicate the critical role of TLR-4 signaling in the development of tissue fibrosis in these models, suggesting that biomolecular TLR-4 targeting is a potential therapeutic approach to SSc.

MATERIALS AND METHODS

Mice. Wild-type (C57BL/6) mice were purchased from Japan SLC. TLR-4$^{-/-}$ and TSK/+ mice (C57BL/6 background) were purchased from The Jackson Laboratory. TLR-4$^{-/-}$;TSK/+ mice were generated by crossing TSK/+ and TLR-4$^{-/-}$ mice. All mice used in this study were female, and mice used in the bleomycin-induced SSc model were 6–8 weeks old at the beginning of treatment with phosphate buffered saline (PBS) or bleomycin. TSK/+ mice were killed at age 8 weeks, and skin and lung sections were excised for histologic evaluation.

Bleomycin treatment. Bleomycin (Nippon Kayaku) was prepared and injected into mice as previously described (24). One group of mice was treated every other day for 3 weeks, and fibrosis was evaluated by histologic analysis. A second group of mice was treated daily for 1 week, and inflammatory cell infiltration, neovascularization, and cytokine expression were analyzed by flow cytometry. Control mice were injected with equal volumes of PBS. All studies and procedures were approved by the Committee on Animal Experimentation of the University of Tokyo Graduate School of Medicine.

Histologic assessment and immunohistochemistry. One day after the final injection, mice were killed, and skin and lung sections were obtained. Sections (6-μm thick) were stained with hematoxylin and eosin, Masson's trichrome stain, and toluidine blue. Dermal and hypodermal thickness were examined as previously described (13,25). Right lungs were excised, and the severity of fibrosis was scored as previously described (25). Immunohistochemistry was performed using antibodies directed against TLR-4 (Imgenex), CD3 (BD PharMingen), B220 (BD PharMingen), F4/80 (Serotec), α-smooth muscle actin (α-SMA; Sigma-Aldrich), CD31 (BD PharMingen), and IL-6 (Abcam). For immunofluorescence staining, serial sections were incubated with antibodies against TLR-4, α-SMA, CD31, and HA (Abcam) as primary antibodies, followed by Alexa Fluor 555–conjugated or fluorescein isothiocyanate–conjugated secondary antibodies (Abcam), corresponding to the primary antibodies. Coverslips were mounted using Vectashield with DAPI (Vector), and staining was examined with Bio Zero BZ-8000 (Keyence). Stained cells were counted in 10 random grids under high-power magnification fields by 2 independent researchers (TT and YA) in a blinded manner.

Collagen measurement. Collagen content of the mouse skin and lung tissues was quantified using QuickZyme Total Collagen Assay according to the recommendations of the manufacturer (QuickZyme Biosciences). Six-mm punch biopsy skin samples and total left lungs were used.

Measurement of cytokines in mouse sera and skin homogenates. Sera were obtained from mice after 3 weeks of treatment with PBS or bleomycin. Total serum IgG, IgM, anti–DNA topoisomerase I antibody, and IL-6 levels were determined by specific enzyme-linked immunosorbent assay (ELISA) kits (for IL-6, R&D Systems; for total IgG and IgM, Abcam; for anti–DNA topoisomerase I antibody, Alpha Diagnostic) following the instructions of the manufacturers. Punched-out lesional skin sections (6 mm) from mice treated with either PBS or bleomycin for 1 week were harvested, homogenized in 300 μl of radioimmunoprecipitation assay

buffer (Santa Cruz Biotechnology), and centrifuged. Lysates were subjected to measurement with specific ELISA kits for IL-6, IL-13, and IL-17A (R&D Systems).

RNA isolation and real-time polymerase chain reaction (PCR). One microgram of RNA was reverse transcribed using an iScript cDNA Synthesis kit (Bio-Rad). Real-time PCR was carried out using SYBR Green PCR Master Mix (Life Technologies) on an ABI Prism 7000 system (Life Technologies) in triplicate. Messenger RNA (mRNA) levels were normalized to those of the GAPDH gene. The primer sequences used are available upon request. The relative change in the levels of genes of interest was determined by the $2^{-\Delta\Delta C_t}$ method. Dissociation analysis for each primer pair was performed to verify specific amplification.

Cell isolation and culture. Mouse dermal fibroblasts were purified as previously described (26). Primary wild-type and TLR-$4^{-/-}$ mouse fibroblasts were passaged once and used for experiments. To obtain dermal microvascular endothelial cells, a cell suspension obtained from dermal collagenase digestion was stained with anti-CD31 microbeads (Miltenyi Biotec) and isolated with magnetic sorting, as previously described (27). Wild-type or TLR-$4^{-/-}$ mouse primary fibroblasts or endothelial cells were seeded at 3×10^4 cells per well and stimulated with 100 ng/ml LPS from *Escherichia coli* (Sigma-Aldrich) for 24 hours to evaluate supernatant IL-6 concentration with a specific ELISA kit (R&D Systems). Macrophages were obtained as previously described (28). Splenic B cells and T cells were isolated with anti-CD19 magnetic-activated cell sorting (MACS) magnetic beads and pan–T cell isolation kit, respectively (Miltenyi Biotech). Cells (5×10^4 per well) were stimulated with 100 ng/ml LPS or left untreated. Supernatants were harvested 24 hours later, and the IL-6 concentration was measured using a specific ELISA kit (R&D Systems). In experiments to determine the production of IL-4, IL-6, and TGFβ1 by purified B cells from PBS-treated or bleomycin-treated mice, mice were treated for 1 week and cells from the draining lymph nodes (i.e., axillary and inguinal lymph nodes) of the lesional skin were subjected to magnetic separation with anti-CD19 MACS beads. The CD19-positive cells were cultured in RPMI medium without stimulation, and after 24 hours, supernatants were harvested and the levels of the cytokines listed above were measured with specific ELISA kits (R&D Systems).

Flow cytometric analysis. Mice were treated with PBS or bleomycin for 1 week. On the day after the final injection, lymphocytes from draining lymph nodes were obtained. In the surface staining experiments, cells were stained with antibodies against B220 (RA3-6B2), CD3 (17A2), F4/80 (BM8), CD11c (N418), and TLR-4 (SA15-21; all from BioLegend). In intracellular cytokine staining, they were stimulated with 10 ng/ml phorbol myristate acetate and 1 μg/ml ionomycin (Sigma-Aldrich) in the presence of 1 μg/ml brefeldin A (GolgiStop; BD PharMingen) for 4 hours. Cells were washed, stained for CD4, treated with fixative/permeabilization buffer (BD PharMingen), and then stained with anti–IL-4 (11B11), anti–IL-17A (TC11.18H10), and anti–interferon-γ (anti-IFNγ) (XMG1.2; all from BioLegend) antibodies. In experiments to analyze transcription factors, antibodies against retinoic acid receptor–related orphan nuclear receptor γt (RORγt) (B2D; eBioscience), T-bet (4B10; BioLegend), and FoxP3 (FJK-16s; eBioscience) were used. Cells were analyzed on a FACSVerse flow cytometer (BD Biosciences). The populations of positive and negative cells were determined using nonreactive isotype-matched antibodies as controls.

Statistical analysis. Data are presented as the mean ± SEM. The Mann-Whitney 2-tailed U test was used for group comparisons. Statistical analysis was carried out using GraphPad Prism. *P* values less than 0.05 were considered significant.

RESULTS

Enhanced expression of TLR-4 and its endogenous ligand in mice treated with bleomycin. We initially evaluated TLR-4 expression in wild-type mice treated with bleomycin. Immunohistochemical staining of the lesional skin and lungs of the mice revealed a significant increase in the number of TLR-4–positive cells after bleomycin treatment (Figures 1A and B). Since the expression of TLR-4 is increased in α-SMA–positive cells and CD31-positive dermal microvascular endothelial cells in the lesional skin of SSc patients (22), we performed double immunofluorescence staining to determine whether TLR-4 expression was increased in these cells in bleomycin-treated mice as well. As shown in Figure 1C, we noted prominently enhanced TLR-4 expression in α-SMA–positive and CD31-positive cells, together with an increased number of these cells, in bleomycin-treated mice compared with control mice. Indeed, a mean ± SEM of 61.8 ± 14.2% and 25.6 ± 8.5% of TLR-4–positive interstitial cells in the bleomycin-treated mice were also positive for α-SMA and CD31, respectively, indicating robust TLR-4 expression in myofibroblasts and endothelial cells. We further examined whether these α-SMA–positive cells expressed endogenous ligands such as HA by double staining for HA and α-SMA. Indeed, there was marked colocalization of these 2 molecules (Figure 1C).

We next performed flow cytometric analysis with cells isolated from the draining lymph nodes of the lesional skin of the mice. Although no difference was seen in dendritic cells, enhanced TLR-4 expression was observed in B cells, T cells, and macrophages in bleomycin-treated mice compared with control mice (Figure 1D). These results indicate that bleomycin increases the expression of TLR-4 in various cell types as well as the expression of endogenous TLR-4 ligands in the lesional skin.

Attenuation of skin fibrosis, inflammatory cell infiltration, and angiogenesis and decreased profibrotic cytokine expression in bleomycin-treated mice with TLR-4 deletion. To evaluate the effect of TLR-4 loss on skin fibrosis, lesional skin sections from mice treated with PBS or bleomycin for 3 weeks were assessed. As

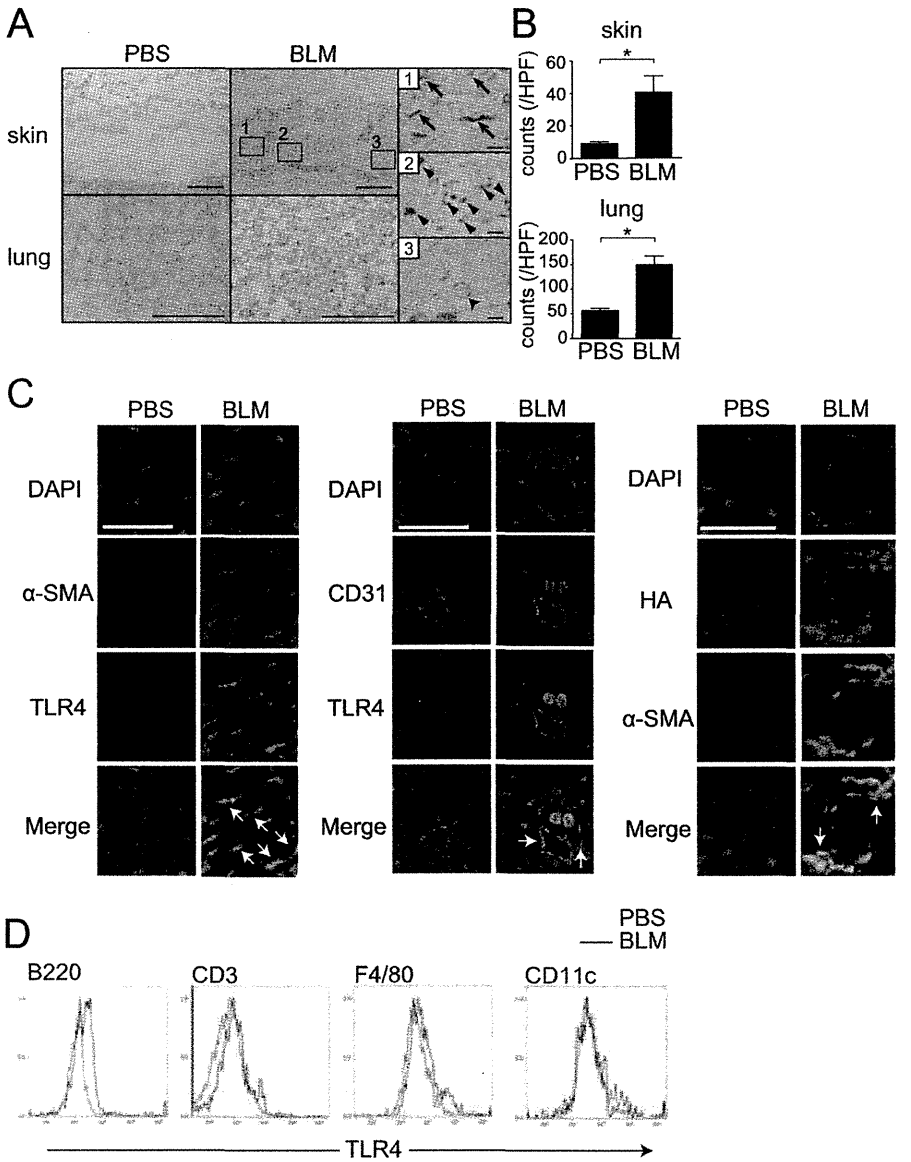

Figure 1. Enhanced expression of Toll-like receptor 4 (TLR-4) and hyaluronic acid (HA) in mice treated with bleomycin (BLM). **A,** Representative images of staining for TLR-4 in sections from the lesional skin and lungs from wild-type mice treated with phosphate buffered saline (PBS) or bleomycin for 3 weeks. The numbered panels show a higher-magnification view of the boxed areas. **Arrows** show TLR-4–positive fibroblasts; **arrowheads** show infiltrating cells; **broken arrow** shows endothelial cells in the skin. Bars = 100 μm in the left and middle panels; bars = 10 μm in the right panels. **B,** Numbers of TLR-4–positive cells in the mouse skin and lungs. Data were quantified by counting positive cells in a ×200 high-power field (hpf). Bars show the mean ± SEM (n = 4–5 mice per group). * = $P < 0.05$. **C,** Representative immunofluorescence images of α-smooth muscle actin (α-SMA)/TLR-4, CD31/TLR-4, and HA/α-SMA double staining in skin samples from mice from each group. **Arrows** indicate double positive cells. Bars = 50 μm. **D,** TLR-4 fluorescence intensity in mononuclear cells from inguinal and axillary lymph nodes from wild-type mice treated with PBS or bleomycin. Cells were gated and costained for B220, CD3, F4/80, CD11c, and TLR-4. Results are representative of 3 experiments.

shown in Figure 2A, the dermal thickness and collagen content were reduced in bleomycin-treated TLR-$4^{-/-}$ mice compared with bleomycin-treated wild-type mice, and the increase in α-SMA positivity was also attenuated

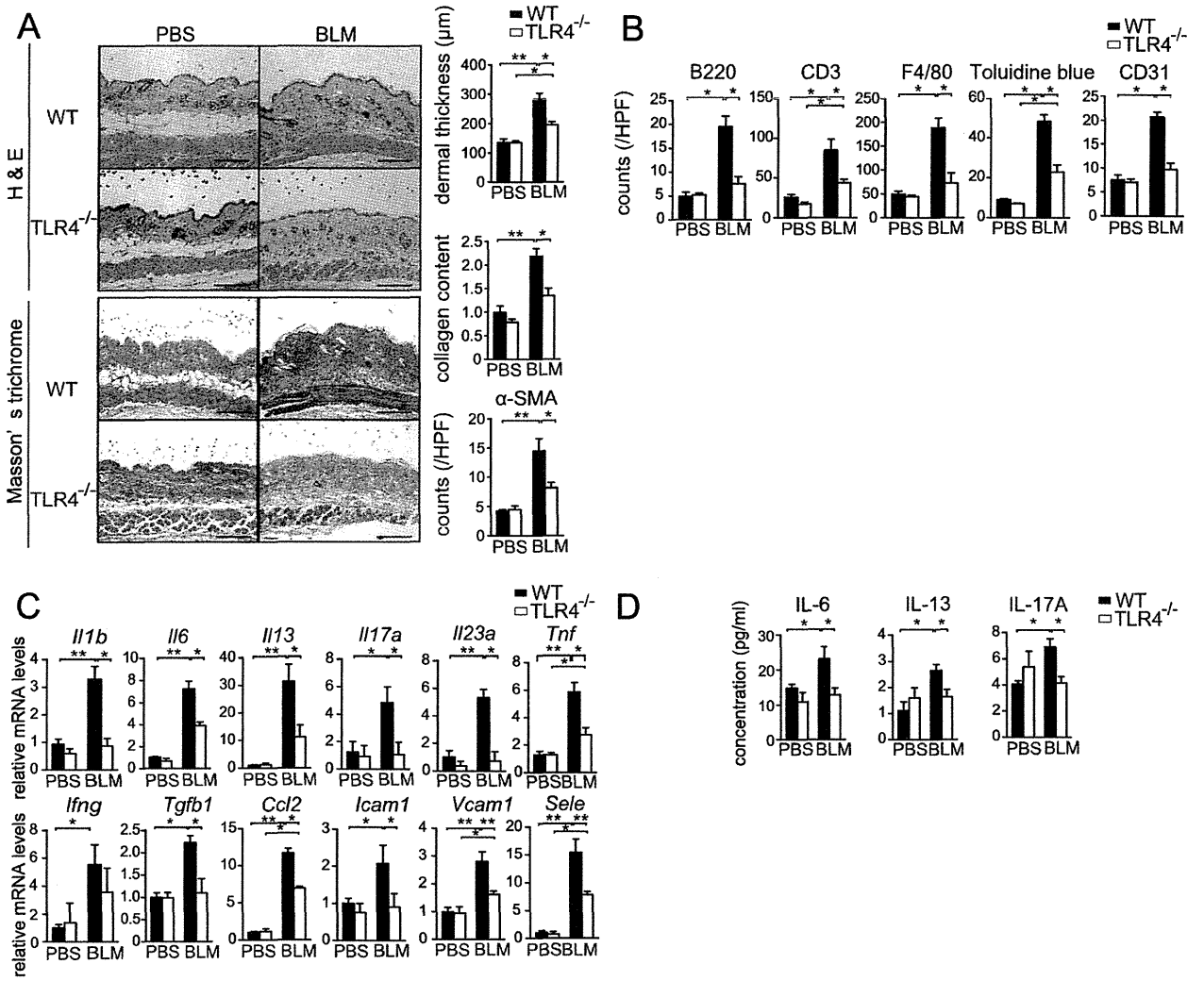

Figure 2. Attenuation of bleomycin-induced fibrosis, inflammatory cell infiltration, angiogenesis, and inflammatory cytokine expression in the lesional mouse skin by TLR-4 deletion. **A,** Left, Representative wild-type (WT) and TLR-4$^{-/-}$ mouse skin sections stained with hematoxylin and eosin (H&E) and Masson's trichrome. Bars = 100 μm. Right, Dermal thickness, collagen content, and α-SMA–positive cells in each group of mice. Values for collagen content are relative to that in PBS-treated wild-type mice (set at 1). **B,** Numbers of B220-positive, CD3-positive, F4/80-positive, toluidine blue–positive, and CD31-positive cells in skin sections from mice treated with PBS or bleomycin for 1 week. **C,** Levels of mRNA for the indicated genes in the lesional mouse skin, assessed by quantitative reverse transcriptase–polymerase chain reaction. **D,** Interleukin-6 (IL-6), IL-3, and IL-17A expression in the lysates of homogenized lesional mouse skin, determined by enzyme-linked immunosorbent assay. One additional independent experiment using another group of mice yielded similar results. Bars show the mean ± SEM (n = 4–8 mice per group in **A, C,** and **D**; n = 4 mice per group in **B**). * = $P < 0.05$; ** = $P < 0.01$. See Figure 1 for other definitions. Color figure can be viewed in the online issue, which is available at http://onlinelibrary.wiley.com/doi/10.1002/art.38901/abstract.

by TLR-4 deletion (Figure 2A). B cell, T cell, macrophage, and mast cell infiltration were markedly increased after bleomycin injection in wild-type mice, while TLR-4$^{-/-}$ mice showed milder infiltration (Figure 2B). In addition, CD31 staining revealed increased vessels in the deep dermis and subcutaneous fat tissue of bleomycin-treated wild-type mice, while TLR-4 knockout attenuated the increase (Figure 2B). Taken together, these results indicate that the activation of TLR-4 signaling plays a vital role in the pathogenic fibrotic processes, including inflammatory cell infiltration and angiogenesis, caused by bleomycin.

We next explored the expression profiles of mRNAs in the lesional mouse skin. Bleomycin treatment increased the levels of mRNA for *Il1b*, *Il6*, *Il13*, *Il17a*, *Il23a*, *Tnf*, *Ifng*, *Tgfb1*, *Ccl2*, *Icam1*, *Vcam1*, and *Sele* genes in wild-type mice, and these increases in mRNA levels were suppressed by TLR-4 deletion (Figure 2C). There were significantly lower protein levels of IL-6, IL-13, and IL-17A in the lesional skin of bleomycin-treated TLR-$4^{-/-}$ mice compared with bleomycin-treated wild-type mice (Figure 2D). These results indicate that TLR-4 is a key molecule required for the expression of soluble factors and cell adhesion molecules that regulate tissue fibrosis in the bleomycin-induced model of SSc.

Reduction in fibrosis and expression of inflammatory cytokines in the lungs of bleomycin-treated TLR-$4^{-/-}$ mice. In addition to skin sclerosis, this bleomycin-induced murine model exhibits lung fibrosis. Histologic analyses revealed less fibrosis and inflammatory cell infiltration in bleomycin-treated TLR-$4^{-/-}$ mice than in bleomycin-treated wild-type mice (Figures 3A and B). Consistent with the findings in the mouse skin, the levels of mRNA for the *Il1b*, *Il6*, *Il13*, *Il23a*, *Tnf*, *Ccl2*, and *Sele* genes were significantly suppressed in bleomycin-treated TLR-$4^{-/-}$ mice compared with bleomycin-treated wild-type mice (Figure 3C), and there was a tendency toward significant suppression of the levels of *Il17a and Tgfb1* by TLR-4 deletion ($P = 0.09$ and $P = 0.06$, respectively) (Figure 3C). These results indicate that TLR-4 signaling plays a pivotal role in pulmonary fibrosis as well by regulating the expression of various soluble factors, growth factors, and cell adhesion molecules in the bleomycin-induced model of SSc.

Reduction in serum IgG, anti–DNA topoisomerase I antibody, and IL-6 levels and attenuated expression of IL-6 in the lesional skin and in vitro with TLR-4 knockout. We next examined the total serum IgG, IgM, anti–DNA topoisomerase I antibody, and IL-6 levels to evaluate the systemic immunologic influence of TLR-4 deletion in this murine model. Consistent with other observations, total serum IgG and IL-6 levels were significantly decreased, and there was a tendency toward a significant decrease in anti–DNA topoisomerase I antibody levels ($P = 0.06$) in bleomycin-treated TLR-$4^{-/-}$ mice compared with their wild-type counterparts (Figure 4A). Considering the pivotal role of IL-6 in the fibrotic process in this disease model as well as in SSc through its direct profibrotic property and immunomodulatory role (29), we next focused on this molecule. Immunostaining for IL-6 in the lesional skin showed increased expression in fibroblasts, endothelial cells, and

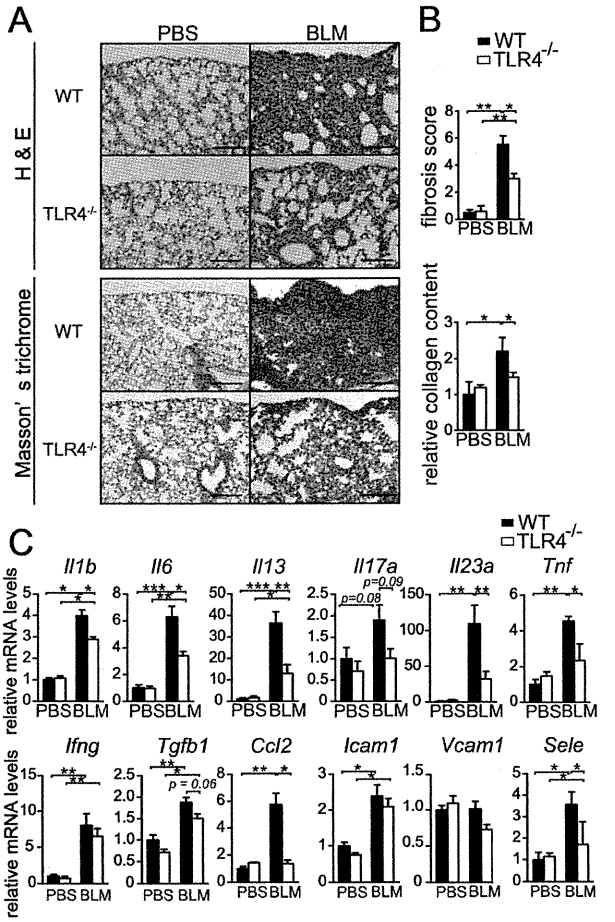

Figure 3. Alleviation of bleomycin-induced inflammatory and fibrotic changes in the mouse lungs by TLR-4 knockout. **A,** Hematoxylin and eosin (H&E) and Masson's trichrome staining of representative lung sections from wild-type (WT) and TLR-$4^{-/-}$ mice injected with PBS or bleomycin. Bars = 100 μm. **B,** Lung fibrosis score and collagen content in each group of mice. Values for collagen content are relative to that in PBS-treated wild-type mice (set at 1). **C,** Levels of mRNA for the indicated genes in the right lungs of the mice, assessed by quantitative reverse transcriptase–polymerase chain reaction. One additional independent experiment using another group of mice yielded similar results. Bars in **B** and **C** show the mean ± SEM (n = 4–8 mice per group). * = $P < 0.05$; ** = $P < 0.01$; *** = $P < 0.001$. See Figure 1 for other definitions. Color figure can be viewed in the online issue, which is available at http://onlinelibrary.wiley.com/doi/10.1002/art.38901/abstract.

perivascular inflammatory cells in bleomycin-treated wild-type mice, while the expression was suppressed in bleomycin-treated TLR-$4^{-/-}$ mice (Figure 4B).

To clarify the impact of TLR-4 loss on IL-6 production, we isolated and stimulated respective cells that are potentially responsible for the decreased IL-6 pro-

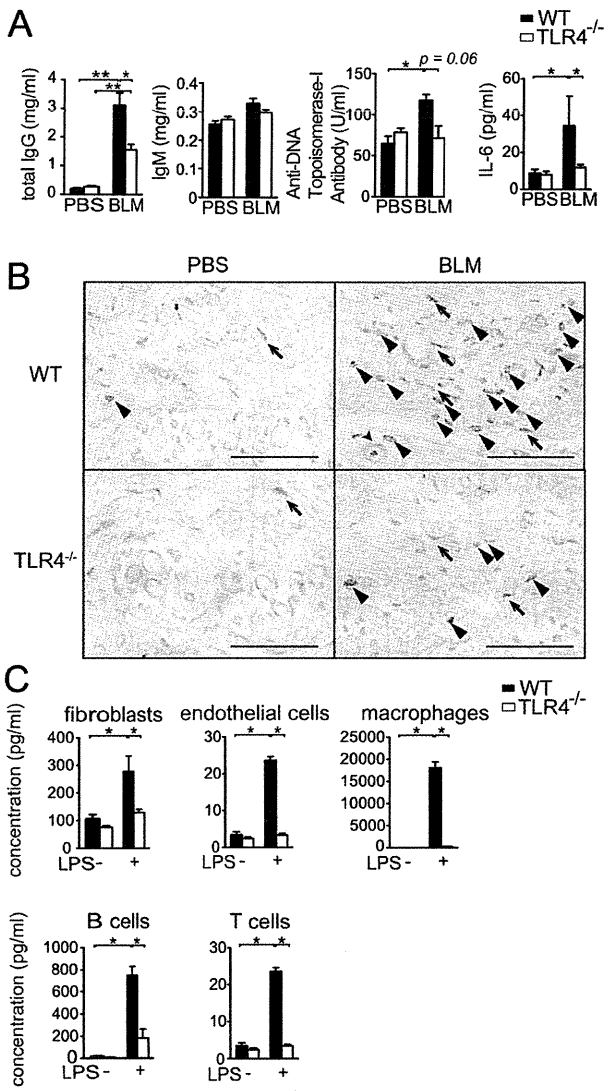

Figure 4. Decreased serum total IgG and anti–DNA topoisomerase I antibody levels and attenuated expression of interleukin-6 (IL-6) in mice with TLR-4 deletion. **A,** Levels of total serum IgG, IgM, anti–DNA topoisomerase I antibody, and IL-6 in wild-type (WT) and TLR-4$^{-/-}$ mice treated with PBS or bleomycin, as determined by enzyme-linked immunosorbent assay (ELISA). **B,** Representative lesional mouse skin sections stained with anti–IL-6 antibody. **Arrows** show IL-6–positive fibroblasts; **arrowheads** show infiltrating cells; **broken arrow** shows endothelial cells. Bars = 50 μm. **C,** Levels of IL-6 in fibroblasts, endothelial cells, macrophages, B cells, and T cells isolated from wild-type and TLR-4$^{-/-}$ mice and left untreated or stimulated with lipopolysaccharide (LPS). Cell culture supernatant was collected, stored, and used for IL-6 measurement by ELISA. One additional independent experiment using another group of mice yielded similar results. Bars in A and C show the mean ± SEM (n = 4–6 mice per group). * = $P < 0.05$; ** = $P < 0.01$. See Figure 1 for other definitions. Color figure can be viewed in the online issue, which is available at http://onlinelibrary.wiley.com/doi/10.1002/art.38901/abstract.

duction in TLR-4$^{-/-}$ mice, namely, fibroblasts, endothelial cells, and inflammatory cells such as macrophages, B cells, and T cells. LPS stimulation of these cells from wild-type mice resulted in a marked increase in IL-6 production in the culture supernatants, while TLR-4 deletion notably suppressed its production (Figure 4C). These results suggest that TLR-4 activation in various cell types by endogenous ligands induced by bleomycin might promote tissue fibrosis in the mouse skin and lungs, at least partly through IL-6 production, which was abrogated by TLR-4 deletion.

Attenuation of bleomycin-induced B cell activation and polarization toward Th2/Th17 in TLR-4$^{-/-}$ mice. Our findings with regard to serum IgG and anti–DNA topoisomerase I antibody led us to examine the systemic immunologic impact of TLR-4 loss on lymphocytes in this disease model. We observed increased numbers of cells in the lesional lymph nodes of wild-type mice treated with bleomycin for 1 week, while bleomycin treatment caused no notable change in TLR-4$^{-/-}$ mice (Figure 5A). B cells purified from the lymph nodes of bleomycin-treated wild-type mice exhibited enhanced production of profibrotic cytokines (IL-4, IL-6, and TGFβ1), while B cells from their TLR-4$^{-/-}$ counterparts showed lower production, indicating attenuated activation of B cells in TLR-4$^{-/-}$ mice (Figure 5B). We then assessed the Th1/Th2/Th17 environment in these diseased mice. Evident polarization toward Th2/Th17 in CD4+ T cells was confirmed by the increased intracellular expression of IL-4 and IL-17A in wild-type mice. However, in TLR-4$^{-/-}$ mice, the increase was attenuated, while the induction of IFNγ was comparable (Figures 5C and D).

We further evaluated master regulators of CD4+ T cell differentiation, such as RORγt for Th17, T-bet for Th1, and FoxP3 for Treg cells. Consistent with the observations described above, while RORγt expression was significantly increased in wild-type mice treated with bleomycin, there was no increase in RORγt expression in bleomycin-treated TLR-4$^{-/-}$ mice. T-bet expression was increased with bleomycin treatment in both wild-type and TLR-4$^{-/-}$ mice, but to a significantly greater extent in TLR-4$^{-/-}$ mice. FoxP3 expression was comparable between bleomycin-treated wild-type mice and bleomycin-treated TLR-4$^{-/-}$ mice (Figure 5D). Thus, these results indicate that TLR-4 signaling is indispensable in the context of B cell activation and Th2/Th17-skewed polarization in the mouse model of bleomycin-induced SSc.

Attenuation of hypodermal fibrosis in TSK/+ mice by TLR-4 knockout. To further explore the impact of TLR-4 knockout in another murine model of SSc, we

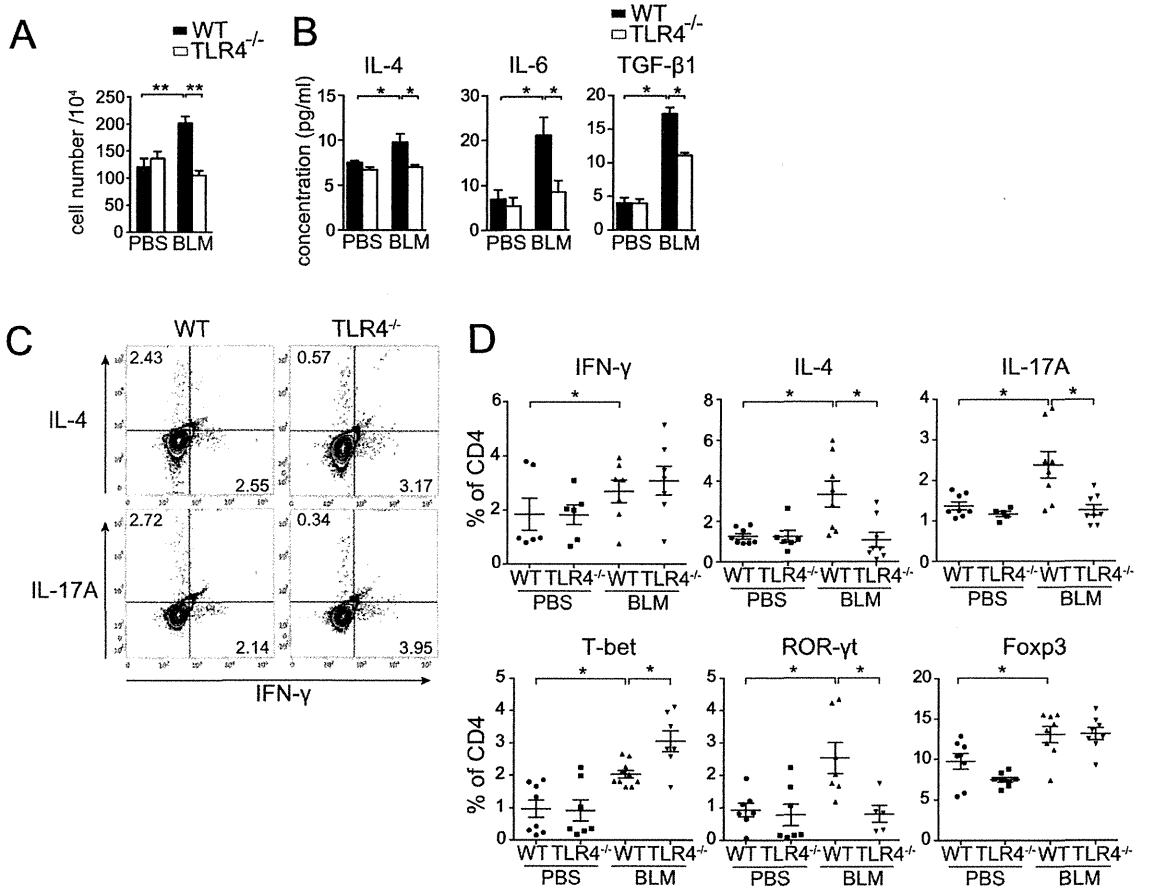

Figure 5. Alleviation of bleomycin-induced B cell activation and skew toward Th2/Th17 milieu in mice after TLR-4 deletion. **A,** Total cell numbers in the bilateral axillary and inguinal lymph nodes of wild-type (WT) and TLR-4$^{-/-}$ mice treated with PBS or bleomycin for 1 week. **B,** Levels of interleukin-4 (IL-4), IL-6, and transforming growth factor β1 (TGFβ1) in B cells purified from the mouse lymph nodes and cultured without stimulation, as determined by enzyme-linked immunosorbent assay. Bars in **A** and **B** show the mean ± SEM (n = 4–8 mice per group in **A**; n = 4–6 mice per group in **B**). * = $P < 0.05$; ** = $P < 0.01$. **C,** Representative fluorescence-activated cell sorting plots of intracellular IL-4, IL-17A, and interferon-γ (IFNγ) staining in CD4+ T cells from the lymph nodes of bleomycin-treated wild-type and TLR-4$^{-/-}$ mice. **D,** Top, Percent of CD4+ cells positive for IFNγ, IL-4, and IL-17A, as determined by intracellular staining. Data were combined from 3 independent experiments. Bottom, Percent of CD4+ cells expressing T-bet, retinoic acid receptor–related orphan nuclear receptor γt (RORγt), and FoxP3. Each data point represents a single mouse; bars show the mean ± SEM (n = 5–8 mice per group for IFNγ, IL-4, and IL-17A; n = 5–10 mice per group for T-bet, RORγt, and FoxP3). * = $P < 0.05$. See Figure 1 for other definitions.

crossed TLR-4$^{-/-}$ mice with TSK/+ mice, a genetic murine model of SSc that is primarily characterized by endogenous activation of fibroblasts (30), generating TLR-4$^{-/-}$;TSK/+ mice. Histologic assessment of hypodermal thickness, the thickness of the subcutaneous loose connective tissue layer, revealed significantly decreased thickness in TLR-4$^{-/-}$;TSK/+ mice compared with control TSK/+ mice (Figure 6A). In contrast to this observation, emphysematous changes in the lungs of TSK/+ mice were not influenced by TLR-4 deletion (Figure 6B). These results suggest the critical roles of TLR-4 signaling in the TSK/+ model as well as in the bleomycin-induced model of SSc, further indicating the importance of TLR-4 in pathologic tissue fibrosis.

DISCUSSION

Extensive studies have shown that TLR-4 is involved in fibrotic processes (31). This study was undertaken to clarify the contribution of TLR-4 signaling to the pathologic fibrosis in SSc murine models.

The pathologic influence of TLR-4 up-regulation

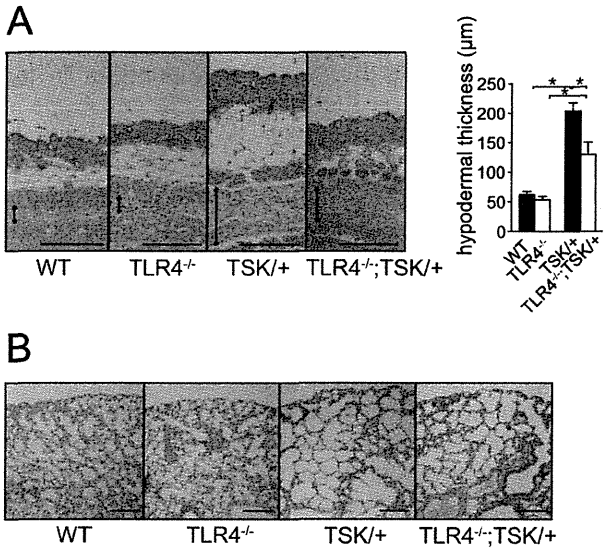

Figure 6. Attenuation of hypodermal fibrosis by Toll-like receptor 4 (TLR-4) deletion in TSK/+ mice. **A,** Left, Representative hematoxylin and eosin (H&E)–stained skin sections from 8-week-old female wild-type (WT), TLR-4$^{-/-}$, TSK/+, and TLR-4$^{-/-}$;TSK/+ mice with hypodermal tissue. **Arrows** indicate hypodermal thickness. Bar = 200 μm. Right, Hypodermal thickness in each mouse group. Bars show the mean ± SEM (n = 4 mice per group). * = $P < 0.05$. **B,** Representative H&E-stained lung sections from the same mice as examined in **A.** Bar = 100 μm. One additional independent experiment using another group of mice yielded similar results. Color figure can be viewed in the online issue, which is available at http://onlinelibrary.wiley.com/doi/10.1002/art.38901/abstract.

has been shown in various chronic inflammatory diseases, and increased TLR-4 signaling alone can break immunologic tolerance (32). However, in the field of SSc research, interest in TLR-4 as a pathogenic factor has focused on the activation of dermal fibroblasts via their own TLR-4 signaling. In this study, consistent with the observation that ~50% and 25% of TLR-4–positive interstitial cells in the SSc lesional dermis were also positive for α-SMA and CD31, respectively (22), our results indicated robust TLR-4 up-regulation in α-SMA–positive and CD31-positive cells, and we further demonstrated enhanced TLR-4 expression in the immune cells from bleomycin-treated mice. Furthermore, we detected enhanced HA production by α-SMA–positive cells that might primarily be myofibroblasts. Using a bleomycin-induced model of lung fibrosis, Li et al showed that this fibrosis is caused by the activated myofibroblasts that actively produce HA (33). Taken together, our results suggest that bleomycin induces TLR-4 activation along with enhanced production of endogenous TLR ligands from these activated cells, and the positive autocrine/paracrine loop that is mediated by TLR-4 might be involved in the pathogenesis of fibrosis in this model.

Our study showed reduced expression of profibrotic mediators in bleomycin-treated TLR-4$^{-/-}$ mice. Previous studies have shown that IL-1β, IL-6, IL-13, IL-17A, TNFα, TGFβ1, MCP-1, intercellular adhesion molecule 1, vascular cell adhesion molecule 1, and E-selectin play essential roles in the pathogenesis of this disease model as well as in SSc (7,8,11,13,24), and their expression levels were significantly decreased by TLR-4 deletion. In addition, infiltration of B cells, T cells, macrophages, and mast cells plays an important role in this model as well as in SSc (34–36). TLR-4 knockdown attenuated infiltration of these cells, and furthermore, suppressed dermal angiogenesis. Since aberrant angiogenesis is also an important disease process in SSc and its murine model (37), it is consistent to observe decreased angiogenesis in TLR-4$^{-/-}$ mice with less fibrosis. Overall, the present study indicates the critical role of TLR-4 to induce the pathologic expression profiles of various soluble factors and cell adhesion molecules and pathologic angiogenesis, which coordinately regulate tissue fibrosis in the murine model of bleomycin-induced SSc and possibly in human SSc.

B cell activation is also a key factor that contributes to the pathogenesis of SSc and its murine models. In addition to the observation that CD19 knockout attenuates bleomycin-induced skin and lung fibrosis in mice (25), recent clinical observations that rituximab, an anti-CD20 antibody, is effective against skin and lung fibrosis in a certain subset of patients with SSc (38), have proven the importance of B cells in SSc. Our observations that TLR-4 abrogation alleviated increased levels of serum total IgG, anti–DNA topoisomerase I antibody, and profibrotic cytokine production by B cells in bleomycin-treated mice suggest the significance of TLR-4–dependent B cell activation in the development of pathologic fibrosis.

IL-6 is a classic profibrotic cytokine that plays pivotal roles in the pathogenesis of SSc and its murine model (11,29), and is produced by various cells including fibroblasts, endothelial cells, B cells, T cells, and macrophages (39). IL-6 enhances collagen synthesis via promoting myofibroblastic differentiation (11). Furthermore, IL-6 drives CD4+ T cells into IL-4–secreting Th2 cells while inhibiting Th1 differentiation and amplifying the profibrotic response (40). In our experiments, reduced IL-6 levels were observed in bleomycin-treated TLR-4$^{-/-}$ mice. The first step of the fibrotic process

might include the generation of TLR-4 endogenous ligands including HA by bleomycin treatment and their autocrine and/or paracrine recognition by TLR-4–expressing cells. This recognition immediately stimulates these cells and enhances the production of this key cytokine, IL-6, thus skewing the Th1/Th2 balance toward Th2 predominance.

Our in vitro data with LPS stimulation showed striking up-regulation of IL-6 in various cell types (e.g., over 100-fold increased induction in macrophages), while there was only modest increase in IL-6 levels by bleomycin treatment in vivo. This discrepancy could be explained by the relatively weak but sustained impact of these endogenous ligands on inflammatory cytokine production relative to LPS, the extremely strong external ligand (41). Importantly, we observed that, in bleomycin-treated TLR-4$^{-/-}$ mice, the degree of reduction in fibrosis paralleled the reduction in IL-6 expression, both of which were roughly half the levels observed in their wild-type counterparts. Therefore, through its direct and indirect impacts on fibrosis, IL-6 might function as an indicator of TLR-4–dependent fibrotic activity. Further exploration of the role and the impact of the TLR endogenous ligands underlying IL-6 induction in pathologic tissue fibrosis is needed.

Previous studies have shown the role of Th2 and Th17 responses in fibrotic diseases including SSc (42). SSc has a distinct Th2 polarization, especially in the early stages of dcSSc. Th2 cells produce key soluble profibrotic mediators, including IL-4, IL-6, and IL-13. Knockdown of T-bet, a master regulator of Th1, results in severer skin sclerosis with bleomycin treatment, and it is almost completely alleviated by IL-13 blockade. Thus, T-bet might serve as a repressor of dermal sclerosis through an IL-13–dependent pathway (8). These findings are consistent with our data showing that T-bet up-regulation was significantly suppressed in more fibrotic bleomycin-treated wild-type mice compared with their less fibrotic TLR-4$^{-/-}$ counterparts. In contrast, IL-13, which was up-regulated with bleomycin treatment, was significantly reduced by TLR-4 knockout. IL-13 is another important Th2 cytokine, and activates tissue fibrosis (43). Furthermore, IL-17A and Th17 cells are the fundamental mediators of autoimmune diseases (44). IL-17A promotes autoimmunity by triggering a positive feedback loop via IL-6 production (45). Bleomycin-induced lung fibrosis is IL-17A dependent (46), and IL-17A abrogation leads to decreased dermal fibrosis in the SSc murine models (13).

Our experiments showed decreased Th2/Th17 response to bleomycin treatment in TLR-4$^{-/-}$ mice, which is compatible with the findings of those previous studies. Since IL-6 mediates the Th17 phenotype (45), it is plausible that decreased IL-6 production in the tissue resulted in less RORγt and IL-17A expression in CD4+ T cells. Taken together, these findings indicate that TLR-4 activation might be critically involved in the differential polarization in Th1/Th2/Th17 balance toward Th2/Th17 and may play important roles in the induction of fibrosis.

Finally, our results revealed significantly decreased hypodermal fibrosis in TLR-4$^{-/-}$;TSK/+ mice compared with TSK/+ mice. The TSK/+ mouse model is a genetic murine model of SSc, which was originally identified with a spontaneous mutation in the *Fbn1* gene coding fibrillin 1 that results in increased synthesis and excessive accumulation of collagen in the skin and visceral organs (30). These mice exhibit elevated TGFβ1 production, and their primary fibroblasts show enhanced collagen production with hypersensitivity to TGFβ1 stimulation (47,48). This model is thus primarily characterized by endogenous activation of fibroblasts, while, on the other hand, it is known to present with a skewed humoral response and produce anti–DNA topoisomerase I antibody (49). CD19 loss significantly attenuates fibrosis in TSK/+ mice, suggesting the important role of B cells in its pathogenesis (49). Furthermore, IL-4 gene disruption rescues TSK/+ mice from skin fibrosis while not from lung emphysema (50), and IL-17A deficiency in TSK/+ mice attenuates skin thickness (13).

Considering that our findings in the bleomycin-induced model of SSc indicate the pivotal role of TLR-4 in B cell activation and in Th2/Th17 skew, which is characterized by IL-4 and IL-17A secretion by T cells, it is possible that TLR-4 deficiency alleviated the fibrosis in TSK/+ mice at least partly through the attenuation of these immunologically pathogenic mechanisms. At the same time, given that TLR-4 signaling augments TGFβ responses and is crucial for fibroblast activation (22), it is also probable that disruption of this signaling attenuated the fibrosis in TSK/+ mice directly through decreased collagen production by fibroblasts with defective TGFβ responsiveness. Further studies are needed to fully elucidate the mechanisms by which TLR-4$^{-/-}$; TSK/+ mice exhibit reduced fibrosis.

There might be a complex interplay of mechanisms leading to fibrosis in SSc, but it became clear that TLR-4 activation is one of the pivotal mechanisms of fibrosis in its murine models. Further investigation is needed to clarify the pathogenesis underlying SSc and the contribution of TLRs.

AUTHOR CONTRIBUTIONS

All authors were involved in drafting the article or revising it critically for important intellectual content, and all authors approved the final version to be published. Dr. Asano had full access to all of the data in the study and takes responsibility for the integrity of the data and the accuracy of the data analysis.

Study conception and design. Takahashi, Asano, Sato.

Acquisition of data. Takahashi.

Analysis and interpretation of data. Takahashi, Asano, Ichimura, Toyama, Taniguchi, Noda, Akamata, Tada, Sugaya, Kadono, Sato.

REFERENCES

1. Asano Y. Future treatments in systemic sclerosis. J Dermatol 2010;37:54–70.
2. Varga J, Abraham D. Systemic sclerosis: a prototypic multisystem fibrotic disorder. J Clin Invest 2007;117:557–67.
3. Sato S, Hasegawa M, Takehara K. Serum levels of interleukin-6 and interleukin-10 correlate with total skin thickness score in patients with systemic sclerosis. J Dermatol Sci 2001;27:140–6.
4. Hasegawa M, Fujimoto M, Kikuchi K, Takehara K. Elevated serum levels of interleukin 4 (IL-4), IL-10, and IL-13 in patients with systemic sclerosis. J Rheumatol 1997;24:328–32.
5. Hasegawa M, Sato S, Takehara K. Augmented production of chemokines (monocyte chemotactic protein-1 (MCP-1), macrophage inflammatory protein-1α (MIP-1α) and MIP-1β) in patients with systemic sclerosis: MCP-1 and MIP-1α may be involved in the development of pulmonary fibrosis. Clin Exp Immunol 1999;117: 159–65.
6. Komura K, Fujimoto M, Hasegawa M, Ogawa F, Hara T, Muroi E, et al. Increased serum interleukin 23 in patients with systemic sclerosis. J Rheumatol 2008;35:120–5.
7. Yamamoto T, Nishioka K. Role of monocyte chemoattractant protein-1 and its receptor, CCR-2, in the pathogenesis of bleomycin-induced scleroderma. J Invest Dermatol 2003;121:510–6.
8. Aliprantis AO, Wang J, Fathman JW, Lemaire R, Dorfman DM, Lafyatis R, et al. Transcription factor T-bet regulates skin sclerosis through its function in innate immunity and via IL-13. Proc Natl Acad Sci U S A 2007;104:2827–30.
9. Sakkas LI, Chikanza IC, Platsoucas CD. Mechanisms of disease: the role of immune cells in the pathogenesis of systemic sclerosis. Nat Clin Pract Rheumatol 2006;2:679–85.
10. Matsushita T, Hasegawa M, Hamaguchi Y, Takehara K, Sato S. Longitudinal analysis of serum cytokine concentrations in systemic sclerosis: association of interleukin 12 elevation with spontaneous regression of skin sclerosis. J Rheumatol 2006;33:275–84.
11. Kitaba S, Murota H, Terao M, Azukizawa H, Terabe F, Shima Y, et al. Blockade of interleukin-6 receptor alleviates disease in mouse model of scleroderma. Am J Pathol 2012;180:165–76.
12. Shima Y, Kuwahara Y, Murota H, Kitaba S, Kawai M, Hirano T, et al. The skin of patients with systemic sclerosis softened during the treatment with anti-IL-6 receptor antibody tocilizumab. Rheumatology (Oxford) 2010;49:2408–12.
13. Okamoto Y, Hasegawa M, Matsushita T, Hamaguchi Y, Le Huu D, Iwakura Y, et al. Potential roles of interleukin-17A in the development of skin fibrosis in mice. Arthritis Rheum 2012;64: 3726–35.
14. Lafyatis R, York M. Innate immunity and inflammation in systemic sclerosis. Curr Opin Rheumatol 2009;21:617–22.
15. Akira S. Toll-like receptor signaling. J Biol Chem 2003;278: 38105–8.
16. Liew FY, Xu D, Brint EK, O'Neill LA. Negative regulation of Toll-like receptor-mediated immune responses. Nat Rev Immunol 2005;5:446–58.
17. Iwasaki A, Medzhitov R. Toll-like receptor control of the adaptive immune responses. Nat Immunol 2004;5:987–95.
18. Marshak-Rothstein A. Toll-like receptors in systemic autoimmune disease. Nat Rev Immunol 2006;6:823–35.
19. Janeway CA Jr, Medzhitov R. Innate immune recognition. Annu Rev Immunol 2002;20:197–216.
20. Yoshizaki A, Komura K, Iwata Y, Ogawa F, Hara T, Muroi E, et al. Clinical significance of serum HMGB-1 and sRAGE levels in systemic sclerosis: association with disease severity. J Clin Immunol 2009;29:180–9.
21. Yoshizaki A, Iwata Y, Komura K, Hara T, Ogawa F, Muroi E, et al. Clinical significance of serum hyaluronan levels in systemic sclerosis: association with disease severity. J Rheumatol 2008;35: 1825–9.
22. Bhattacharyya S, Kelley K, Melichian DS, Tamaki Z, Fang F, Su Y, et al. Toll-like receptor 4 signaling augments transforming growth factor-β responses: a novel mechanism for maintaining and amplifying fibrosis in scleroderma. Am J Pathol 2013;182:192–205.
23. McElwee KJ, Hoffmann R. Alopecia areata: animal models. Clin Exp Dermatol 2002;27:410–7.
24. Yoshizaki A, Yanaba K, Iwata Y, Komura K, Ogawa A, Akiyama Y, et al. Cell adhesion molecules regulate fibrotic process via Th1/Th2/Th17 cell balance in a bleomycin-induced scleroderma model. J Immunol 2010;185:2502–15.
25. Yoshizaki A, Iwata Y, Komura K, Ogawa F, Hara T, Muroi E, et al. CD19 regulates skin and lung fibrosis via Toll-like receptor signaling in a model of bleomycin-induced scleroderma. Am J Pathol 2008;172:1650–63.
26. Gallucci RM, Sloan DK, Heck JM, Murray AR, O'Dell SJ. Interleukin 6 indirectly induces keratinocyte migration. J Invest Dermatol 2004;122:764–72.
27. Cassoni P, Marrocco T, Bussolati B, Allia E, Munaron L, Sapino A, et al. Oxytocin induces proliferation and migration in immortalized human dermal microvascular endothelial cells and human breast tumor-derived endothelial cells. Mol Cancer Res 2006;4: 351–9.
28. Zeini M, Traves PG, Lopez-Fontal R, Pantoja C, Matheu A, Serrano M, et al. Specific contribution of p19(ARF) to nitric oxide-dependent apoptosis. J Immunol 2006;177:3327–36.
29. Khan K, Xu S, Nihtyanova S, Derrett-Smith E, Abraham D, Denton CP, et al. Clinical and pathological significance of interleukin 6 overexpression in systemic sclerosis. Ann Rheum Dis 2012;71:1235–42.
30. Green MC, Sweet HO, Bunker LE. Tight-skin, a new mutation of the mouse causing excessive growth of connective tissue and skeleton. Am J Pathol 1976;82:493–512.
31. Seki E, De Minicis S, Osterreicher CH, Kluwe J, Osawa Y, Brenner DA, et al. TLR4 enhances TGF-β signaling and hepatic fibrosis. Nat Med 2007;13:1324–32.
32. Liu B, Yang Y, Dai J, Medzhitov R, Freudenberg MA, Zhang PL, et al. TLR4 up-regulation at protein or gene level is pathogenic for lupus-like autoimmune disease. J Immunol 2006;177:6880–8.
33. Li Y, Jiang D, Liang J, Meltzer EB, Gray A, Miura R, et al. Severe lung fibrosis requires an invasive fibroblast phenotype regulated by hyaluronan and CD44. J Exp Med 2011;208:1459–71.
34. Kraaij MD, van Laar JM. The role of B cells in systemic sclerosis. Biologics 2008;2:389–95.
35. Yamamoto T, Takagawa S, Katayama I, Yamazaki K, Hamazaki Y, Shinkai H, et al. Animal model of sclerotic skin. I. Local injections of bleomycin induce sclerotic skin mimicking scleroderma. J Invest Dermatol 1999;112:456–62.
36. Ishikawa O, Ishikawa H. Macrophage infiltration in the skin of patients with systemic sclerosis. J Rheumatol 1992;19:1202–6.
37. Yamamoto T, Katayama I. Vascular changes in bleomycin-induced scleroderma. Int J Rheumatol 2011;2011:270938.
38. Jordan S, Distler JH, Maurer B, Huscher D, van Laar JM, Allanore Y, et al. Effects and safety of rituximab in systemic sclerosis: an analysis from the European Scleroderma Trial and

Research (EUSTAR) group. Ann Rheum Dis 2014. E-pub ahead of print.
39. Akira S, Hirano T, Taga T, Kishimoto T. Biology of multifunctional cytokines: IL 6 and related molecules (IL 1 and TNF). FASEB J 1990;4:2860–7.
40. Rincon M, Anguita J, Nakamura T, Fikrig E, Flavell RA. Interleukin (IL)-6 directs the differentiation of IL-4-producing CD4+ T cells. J Exp Med 1997;185:461–9.
41. Akbarshahi H, Axelsson JB, Said K, Malmstrom A, Fischer H, Andersson R. TLR4 dependent heparan sulphate-induced pancreatic inflammatory response is IRF3-mediated. J Transl Med 2011;9:219.
42. O'Reilly S, Hugle T, van Laar JM. T cells in systemic sclerosis: a reappraisal. Rheumatology (Oxford) 2012;51:1540–9.
43. Kaviratne M, Hesse M, Leusink M, Cheever AW, Davies SJ, McKerrow JH, et al. IL-13 activates a mechanism of tissue fibrosis that is completely TGF-β independent. J Immunol 2004;173: 4020–9.
44. Korn T, Bettelli E, Oukka M, Kuchroo VK. IL-17 and Th17 cells. Annu Rev Immunol 2009;27:485–517.
45. Ogura H, Murakami M, Okuyama Y, Tsuruoka M, Kitabayashi C, Kanamoto M, et al. Interleukin-17 promotes autoimmunity by triggering a positive-feedback loop via interleukin-6 induction. Immunity 2008;29:628–36.
46. Wilson MS, Madala SK, Ramalingam TR, Gochuico BR, Rosas IO, Cheever AW, et al. Bleomycin and IL-1β-mediated pulmonary fibrosis is IL-17A dependent. J Exp Med 2010;207:535–52.
47. Jimenez SA, Williams CJ, Myers JC, Bashey RI. Increased collagen biosynthesis and increased expression of type I and type III procollagen genes in tight skin (TSK) mouse fibroblasts. J Biol Chem 1986;261:657–62.
48. Zhu H, Bona C, McGaha TL. Polymorphisms of the TGF-β1 promoter in tight skin (TSK) mice. Autoimmunity 2004;37:51–5.
49. Saito E, Fujimoto M, Hasegawa M, Komura K, Hamaguchi Y, Kaburagi Y, et al. CD19-dependent B lymphocyte signaling thresholds influence skin fibrosis and autoimmunity in the tight-skin mouse. J Clin Invest 2002;109:1453–62.
50. Kodera T, McGaha TL, Phelps R, Paul WE, Bona CA. Disrupting the IL-4 gene rescues mice homozygous for the tight-skin mutation from embryonic death and diminishes TGF-β production by fibroblasts. Proc Natl Acad Sci U S A 2002;99:3800–5.

JAPANESE DERMATOLOGICAL ASSOCIATION
THE JOURNAL OF DERMATOLOGY
doi: 10.1111/1346-8138.13030
Journal of Dermatology 2015; **42**: 1–7

ORIGINAL ARTICLE

Beneficial effect of botulinum toxin A on Raynaud's phenomenon in Japanese patients with systemic sclerosis: A prospective, case series study

Sei-ichiro MOTEGI,[1] Kazuya YAMADA,[1] Sayaka TOKI,[1] Akihiko UCHIYAMA,[1] Yuka KUBOTA,[2] Tetsuya NAKAMURA,[2] Osamu ISHIKAWA[1]

[1]*Department of Dermatology,* [2]*Clinical Investigation and Research Unit, Gunma University Graduate School of Medicine, Maebashi, Japan*

ABSTRACT

Currently, there is no satisfactory treatment for Raynaud's phenomenon (RP) in systemic sclerosis (SSc). Recently, it has been reported that botulinum toxin A (BTX-A) injection was effective for the treatment of RP in SSc patients. The objective was to assess the efficacy and safety of BTX-A on RP in Japanese SSc patients. In the prospective, case series study, 10 Japanese SSc patients with RP received 10 U of BTX-A injections into the hand. The change in severity of RP, including the frequency of attacks/pain, color changes, duration time of RP and the severity of pain, was assessed by Raynaud's score and pain visual analog scale (VAS) at each visit during 16 weeks. The recovery of skin temperature 20 min after cold water stimulation was examined by thermography at baseline and 4 weeks after injection. The number of digital ulcers (DU) and adverse effects were assessed at each visit. BTX-A injection decreased Raynaud's score and pain VAS from 2 weeks after injection, and the suppressive effect was continued until 16 weeks after injection. Skin temperature recovery after cold water stimulation at 4 weeks after injection was significantly enhanced compared with that before injection. All DU in five patients were healed within 12 weeks after injection. Neither systemic nor local adverse effects were observed in all cases. We conclude that BTX-A injection significantly improved the activity of RP in SSc patients without any adverse events, suggesting that BTX-A may have possible long-term preventive and therapeutic potentials for RP in Japanese SSc patients.

Key words: **botulinum toxin A, digital ulcer, Raynaud's phenomenon, systemic sclerosis.**

INTRODUCTION

Systemic scleroderma (SSc) is a generalized connective tissue disease characterized by fibrosis of the skin and internal organs, vascular dysfunction and immune disorder.[1–4] Patients with SSc typically develop Raynaud's phenomenon (RP) and persistent digital ischemia, and often develop digital ulcers (DU). We previously reported that the demographic and clinical features of SSc patients showed that young age, male sex, anti-topoisomerase I antibody positivity, severe skin sclerosis, interstitial lung disease complication and cardiac involvements were significantly prevalent in patients with vasculopathy, such as RP and DU.[4]

Raynaud's phenomenon is characterized by the presence of episodic vasospasms of the peripheral blood vessels and ischemia of fingers in response to cold or emotional stress. The pathogenesis of RP in SSc is complex and unknown. Several neurotransmitters and their receptors, which regulate vasoconstriction and vasodilation, are implicated in the pathogenesis of RP.[5] It has been considered that cold- or stress-induced norepinephrine stimulates the adrenergic receptor (AR) α on pericytes and/or vascular smooth muscle cells, thus resulting in vasoconstriction.[5,6] In addition, the ARα response are increased in the digital arteries in SSc patients,[7] suggesting that norepinephrine is involved in the pathogenesis of RP in SSc. Norepinephrine and other neurotransmitters, including substance P, glutamate and calcitonin gene-related peptide, are increased in peripheral nerves of the affected skin and induce severe pain and paresthesia of fingers in patients with RP.[8–12]

It has also been considered that episodic vasospasms may result from the dysregulation of vasoconstriction and vasodilation, and ischemia–reperfusion (I/R) injury may be involved in the pathogenesis of the symptoms of RP, such as severe pain and paresthesia of the fingers, as well as the development of DU. I/R injury is identified as the reperfusion of blood to previously ischemic tissue, which induces excessive cellular injury.[13,14] The infiltration of inflammatory cells and the production of pro-inflammatory cytokines are induced by reperfusion of blood into a hypoxic tissue, resulting in damage to the

Correspondence: Sei-ichiro Motegi, M.D., Ph.D., Department of Dermatology, Gunma University Graduate School of Medicine, 3-39-22 Showa, Maebashi, Gunma 371-8511, Japan. Email: smotegi@gunma-u.ac.jp
Received 4 June 2015; accepted 11 June 2015.

vascular endothelium, edema, capillary narrowing and apoptosis and necrosis of tissues.[15,16]

Because RP in SSc patients can lead to DU and gangrene, urgent medical intervention is required. Pharmacological treatments of RP have targeted the enhancement of vasodilation and/or reduction of vasoconstriction, such as calcium channel blockers, antiplatelet agents (including aspirin), sarpogrelate hydrochloride (a serotonin receptor antagonist), cilostazol (a phosphodiesterase inhibitor), and oral and i.v. prostanoid, (including beraprost sodium, a prostaglandin I_2 analog, and lipoprostaglandin E_1). The endothelin receptor antagonists bosentan and phosphodiesterase-5 inhibitor may benefit functional impairment in SSc-related RP patients.[17,18] However, no satisfactory treatments for RP in SSc currently exist. Several studies have recently shown the beneficial effects of botulinum toxin A (BTX-A) on RP in patients with SSc, and these have been reviewed.[19–27] SSc patients with RP were injected with BTX-A at a dose ranging 10–100 U per hand on each neurovascular bundle at the level of the metacarpophalangeal joint. Raynaud's symptom severity was assessed using Raynaud's score and the visual analog scale (VAS) for pain. The majority reported an improvement in severe resting pain and a reduction in the frequencies of RP. BTX-A injection increased the digital blood flow as assessed using laser Doppler imaging. DU was also healed after BTX-A injection. Hand functions, such as pinch and power grip, ranges of movement and disabilities of arm, shoulder and hand, were improved by BTX-A.[26] There were a few adverse effects, such as intrinsic weakness and dysesthesia. However, these symptoms disappeared within 2–5 months after treatment. In the present study, we examined the efficacy and safety of the administration of BTX-A on RP in Japanese patients with SSc.

METHODS

Study design

This study was designed as a prospective, case series study. It was initiated in November 2014 and conducted over the cold winter months from 2014 to 2015 to maximize the development of RP, as well as to minimize the seasonal effects on RP. This study was performed at the Department of Dermatology, and Clinical Investigation and Research Unit, Gunma University. This study was approved by the institutional review board of Gunma University. All patients provided their written informed consent before participation. Treatment was started at day 0 (baseline) and reviewed at weeks 2, 4, 8, 12 and 16. The primary outcome was the change in severity of RP, including the frequency, pain, color and duration, according to Raynaud's score and the VAS at 4 weeks after treatment compared with the baseline values. The secondary outcome was the changes of the temperature differences of the tip of the treated finger between just after cold water challenge and 20 min later by thermography at each visit. The changes of the number of DU during 16 weeks, and the changes in the severity of RP according to Raynaud's score and the VAS at 2, 8, 12 and 16 weeks after treatment compared with the baseline were also considered as secondary outcome variables. Adverse effects were reviewed at each visit.

Patients

Ten Japanese patients (three men, seven women; mean age ± standard error, 62.5 ± 3.5 years) with SSc were treated with BTX-A. All patients fulfilled the criteria of SSc proposed by the American College of Rheumatology (1980)[28] and the American College of Rheumatology/European League Against Rheumatism Classification Criteria (2013).[29] Four patients were classified into the limited cutaneous type (lcSSc) and six patients were classified into the diffuse cutaneous type (dcSSc) of SSc according to the classification by LeRoy *et al.*[30] Skin sclerosis was assessed using the modified Rodnan total skin score (mRTSS), and the average mRTSS was 11.6 ± 1.9 (range, 6–26). Five patients had DU on the tip of their fingers at baseline. All patients had a history of severe RP for various periods and had taken oral prostanoid, beraprost sodium and/or antiplatelet agents, such as sarpogrelate hydrochloride or cilostazol. Patients with DU were additionally treated with an i.v. prostanoid, including lipoprostaglandin E_1. However, these therapies were not effective and severe RP and DU persisted before BTX-A treatment. Patients under 18 years of age, with pregnancy or having previous medical histories of BTX-A treatment were excluded.

Treatment and evaluation protocol

Only one finger with the most severe symptoms was selected, and BTX-A was injected into both sides of the selected finger. Each 50-unit vial of BTX-A (BOTOX VISTA; Allergan Pharmaceuticals, Irvine, CA, USA) was diluted in 2.5 mL saline (20 U/mL), and 0.5 mL (10 U) of BTX-A was injected s.c. into the palmar aspect of the hand, just proximal to the A1 pulley, targeting the neurovascular bundles using a 30-G needle (Fig. 1a; injection points are indicated by black marker). The change in the severity of RP, including the frequency, pain, color and duration, was assessed using Raynaud's score.[31,32] Raynaud's score is the modified Raynaud's condition score[33] and an assessment of the RP activity (range, 0–16), including the frequency of attacks (0 = none, 1 = once per 2 weeks, 2 = once per week, 3 = once per 2 days, 4 = every day), pain (0 = none, 1 = fairly rare, 2 = rare, 3 = sometimes, 4 = always), color (0 = none, 1 = red, 2 = purple, 3 = sometimes white, 4 = always white) and duration time of RP (0 = none, 1 = within 15 min, 2 = between 15 and 30 min, 3 = between 30 and 60 min, 4 = >60 min). The total score at baseline was identified as 100% and the relative scores at each visit were quantified. Pain severity was assessed using the 100-mm VAS (range, 0–100; 0 = no pain, 100 = pain as bad as imaginable).[34] To assess the recovery of skin temperature in the treated finger, the skin temperature of the tip of the finger was measured just after and 20 min after an ice-bath immersion. At first, both hands were put into cold water (12°C in water bath) for 5 min. Both hands were pulled out from the cold water, and then the skin temperature of the tip of the treated finger was measured using thermography at controlled room temperature (26°C). Twenty minutes later, the skin temperature of the

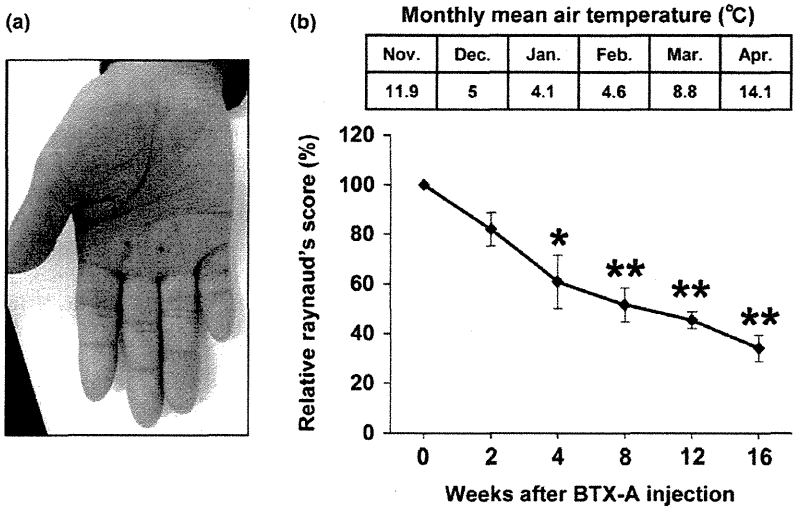

Figure 1. Botulinum toxin A (BTX-A) injection improved the symptoms of Raynaud's phenomenon in systemic sclerosis patients. (a) BTX-A was injected s.c. into the palmar aspect of the hand (indicated by black marker), just proximal to the A1 pulley, targeting the neurovascular bundles. (b) The average temperature in our city from December 2014 to March 2015. The mean values of Raynaud's score before and after BTX-A injection during 16 weeks. The value of Raynaud's score at baseline was assigned a value of 100%. Values were determined in $n = 10$ patients. $^{**}P < 0.01$, $^{*}P < 0.05$ relative to baseline value.

tip of the treated finger was also recorded, and the difference of the temperatures between just after the cold water challenge and 20 min later was calculated. This skin temperature measurement was performed at each visit. The changes in the number of DU were also assessed during the 16-week period.

Statistics

P-values were calculated using one-way ANOVA followed by Dunnett's post-hoc test or Tukey's post-hoc test as appropriate. Error bars represent the standard errors of the mean.

RESULTS

BTX-A injection improved the symptoms of RP in SSc patients

Ten SSc patients with RP received BTX-A injection into the hand during November 2014 to early January 2015. Because cold temperature is an aggravating factor of RP, the symptoms of RP in SSc patients, including frequency, pain and duration, were typically exacerbated during winter in our city in Japan. The average temperature in our city was below 10°C from December 2014 to March 2015 (Fig. 1b).[35] BTX-A injection decreased Raynaud's score from 2 weeks after injection and significantly reduced the score from 4 to 16 weeks after injection (Fig. 1b). These results suggest that BTX-A injection may improve the activity of RP, including the frequency of attacks/pain, color changes and duration time of RP.

BTX-A injection improved the pain of RP in SSc patients

Next, we examined the changes of pain due to RP attack using the pain VAS. BTX-A injection significantly decreased the pain VAS at 2 weeks after injection, and this inhibition effect continued until 16 weeks after injection (Fig. 2). These results suggest that BTX-A injection may improve severe RP pain.

BTX-A injection enhanced the skin temperature recovery after cold water stimulation

Van Beek *et al.*[20] reported the increase in skin surface temperature of 1–4°C within 2–7 days after BTX-A injection. We also

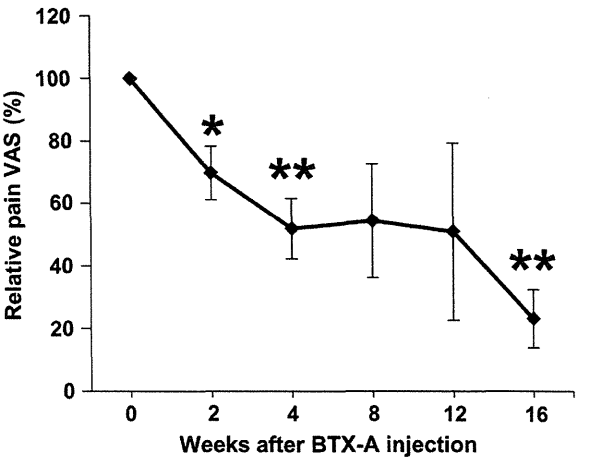

Figure 2. Botulinum toxin A (BTX-A) injection improved the pain of Raynaud's phenomenon in systemic sclerosis patients. The mean values of pain visual analog scale (VAS) before and after BTX-A injection during 16 weeks. The value of pain VAS at baseline was assigned a value of 100%. Values were determined in $n = 10$ patients. $^{**}P < 0.01$, $^{*}P < 0.05$ relative to baseline value.

examined the skin surface temperature before and after injection using thermography. To avoid the effect of air temperature, we measured the differences of temperature between just after and 20 min after cold water stimulation. Our results showed that the skin surface temperature recovery after cold water stimulation at 4 weeks after injection was significantly enhanced compared with that before injection (Fig. 3a). A thermographic image at 10 min after cold water stimulation at 4 weeks after BTX-A injection showed that the skin temperature in the BTX-A injected finger (right index finger) and fingers next to the injected finger (right thumb and middle finger) was significantly elevated compared with that in the other fingers (Fig. 3b). These results suggest that BTX-A injection may enhance the digital blood flow, resulting in an enhancement of the skin surface temperature recovery after cold water stimulation.

RP-related intractable DU were healed after BTX-A injection

Five SSc patients with RP had intractable DU on the tip of the finger treated by BTX-A at baseline. All patients with DU had been treated by oral or i.v. prostanoid and antiplatelet agents for several weeks, but not healed. Although DU were generally exacerbated during winter, a DU in one patient healed at 2 weeks after BTX-A injection, and all DU in five patients were healed within 12 weeks after injection (Fig. 4a). A representative result of BTX-A treatment against DU showed that a DU on the tip of the finger of one SSc patient with RP at baseline was healed 4 weeks after BTX-A injection (Fig. 4b). These results suggest that BTX-A injection may affect the healing of RP-related intractable DU.

Importantly, no systemic or local adverse events of BTX-A were observed in any of our cases. The patients had pain at the injection sites, however, this pain was resolved within a few days. Additionally, a reduction in muscle contraction force was not observed.

DISCUSSION

Botulinum toxin is a polypeptide produced by the bacterium *Clostridium botulinum*, which contains a protease that plays an active role in inhibiting acetylcholine release at the neuromuscular junction and the eccrine sweat glands. There are seven (A–G) serotypes of BTX, and type A has been extensively studied and clinically used. BTX-A treatment has wide therapeutic applications and its use is indicated for blepharospasm, facial spasms, cervical dystonia, spasms of the extremities, esthetic indications of facial wrinkles and axial hyperhidrosis. In addition, there is a broad spectrum of other indications for migraine, achalasia, urinary bladder dysfunction and anal fissures.[36–40]

Several reports demonstrated that BTX-A enhanced the blood flow and survival of ischemic skin flaps using animal cutaneous flap models,[41–44] suggesting that BTX-A-induced acetylcholine-mediated vascular smooth muscle paralysis may inhibit spasm and vascular contraction as well as increase the blood flow. This mechanism is thought to contribute to the improvement of RP by BTX-A.

Another mechanism is thought to be due to the fact that BTX-A can block the release of norepinephrine and inhibit the expression of AR in the vessel walls.[23,25] This mechanism by BTX-A leads to reduced vasoconstriction and pain. In addition, it has been reported that the surface expression of ARα is enhanced by reactive oxygen species (ROS) produced in smooth muscle cells in response to cooling.[45,46] Our previous study demonstrated that BTX-A reduced oxidant-induced intracellular accumulation of ROS in vascular endothelial cells *in vitro*.[47] These results suggest that the antioxidant effect of BTX-A may participate in the beneficial effect of BTX-A on RP in SSc patients. Our results showed that BTX-A injection enhanced the recovery of skin temperature after cold water stimulation, suggesting that BTX-A may suppress vasoconstriction caused by cold-induced norepinephrine and the surface expression of ARα.

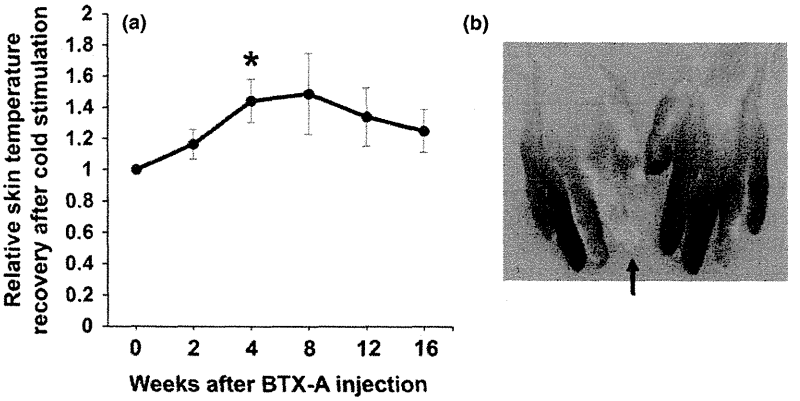

Figure 3. Botulinum toxin A (BTX-A) injection enhanced the skin temperature recovery after cold water stimulation. (a) The mean values of skin surface temperature recovery after cold water stimulation before and after BTX-A injection during 16 weeks. The value of skin surface temperature recovery at baseline was assigned a value of 100%. Values were determined in $n = 10$ patients. $^*P < 0.05$ relative to baseline value. (b) Thermographic image at 10 min after cold water stimulation at 4 weeks after BTX-A injection. BTX-A injected finger (right index finger) is indicated by arrow.

(a)

Weeks	0	2	4	8	12	16
Rate of patients with DU (%)	100 (5/5)	80 (4/5)	40 (2/5)	20 (1/5)	0 (0/5)	0 (0/5)

(b)

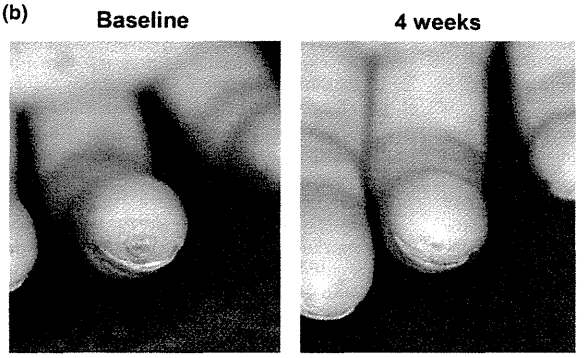

Figure 4. Raynaud's phenomenon (RP)-related intractable digital ulcers (DU) were healed after botulinum toxin A (BTX-A) injection. (a) Rate of patients with DU after BTX-A injection during 16 weeks. The rate of patients with DU at baseline was assigned a value of 100%. (b) DU on the tip of the finger of systemic sclerosis patient with RP at baseline and 4 weeks after BTX-A injection.

Furthermore, BTX-A can block the release of various neuropeptides, such as calcitonin gene-related peptide, glutamate and substance P, which increase in chronic nerve irritation and pain and can exacerbate these symptoms.[10,12,48,49] In addition, Neumeister *et al.*[23] suggested that BTX-A may reduce pain through the inhibition of ectopic sodium channels expressed in chronically irritated or injured nerves by chronic ischemia in patients with RP. Thus, their findings suggest that BTX-A could reduce pain and paresthesia in the fingers by blocking the release of pain-related neuropeptides and the inhibition of its receptors.

We recently demonstrated the beneficial effects of BTX-A against an intermittent short-time cutaneous I/R injury mimicking RP-induced ulcers using an experimental murine model, suggesting that the exogenous application of BTX-A may have therapeutic potential for cutaneous I/R injuries, including RP.[47] BTX-A injection prevented skin ulcer formation after cutaneous I/R injury by protecting against the reduction of vascularity by I/R injury, reducing the hypoxic area, oxidative stress and apoptosis of cells *in vivo* and reducing oxidative stress-induced ROS in vascular endothelial cells *in vitro*. Based on these findings, the protective effect of BTX-A against I/R injury may also contribute to the beneficial effect of BTX-A on RP.

To the best of our knowledge, this is the first investigation to examine the effects of BTX-A injection on RP in Japanese SSc patients. Our findings demonstrated that BTX-A injection significantly improved the activity of RP, including the frequency of attacks/pain, color changes, duration time of RP and the severity of pain. Collectively, BTX-A injection revealed a beneficial therapeutic effect on RP in Japanese SSc patients. The clinical effectiveness of BTX-A has been reported to last for at least 3–6 months in humans.[19–26] According to our results, the beneficial effects of BTX-A continued for at least 4 months after injection. Because warm temperature also improves RP, we did not know the precise effect of BTX-A at 16 weeks after injection. However, we think that SSc patients with RP could avoid severe exacerbation of RP-associated symptoms during winter by one-time BTX-A injection.

Botulinum toxin A is already used in a variety of clinical applications without any significant adverse events. In our study, BTX-A significantly improved the symptoms of RP in SSc patients without any adverse events, suggesting that exogenous BTX-A administration may have possible long-term preventive and therapeutic potentials for RP secondary to SSc and primary RP. However, our study and previous studies have several limitations, such as a small sample size, the lack of controls and the varying severity of RP. Therefore, larger double-blind, prospective, randomized, placebo-controlled studies are warranted to elucidate the beneficial efficacy of BTX-A on the symptoms of RP.

ACKNOWLEDGMENT: This work was supported by the Science Research Grant of Project for Securing High Quality Clinical Research (Gunma University Hospital), institutions selected by the Japanese Ministry of Health, Labor and Welfare in fiscal year 2013, Japan (to T. N.).

CONFLICT OF INTEREST: The authors declare there are no conflicts of interest.

REFERENCES

1 Asano Y. Future treatments in systemic sclerosis. *J Dermatol* 2010; **37**: 54–70.

2 Jinnin M. Mechanisms of skin fibrosis in systemic sclerosis. *J Dermatol* 2010; **37**: 11–25.
3 Hamaguchi Y, Hasegawa M, Fujimoto M *et al.* The clinical relevance of serum antinuclear antibodies in Japanese patients with systemic sclerosis. *Br J Dermatol* 2008; **158**: 487–495.
4 Motegi S, Toki S, Hattori T, Yamada K, Uchiyama A, Ishikawa O. No association of atherosclerosis with digital ulcers in Japanese patients with systemic sclerosis: evaluation of carotid intima-media thickness and plaque characteristics. *J Dermatol* 2014; **41**: 604–608.
5 Herrick AL. The pathogenesis, diagnosis and treatment of Raynaud phenomenon. *Nat Rev Rheumatol* 2012; **8**: 469–479.
6 Wigley FM. Clinical practice Raynaud's phenomenon. *N Engl J Med* 2002; **347**: 1001–1008.
7 Flavahan NA, Flavahan S, Liu Q *et al.* Increased alpha2-adrenergic constriction of isolated arterioles in diffuse scleroderma. *Arthritis Rheum* 2000; **43**: 1886–1890.
8 Chung K, Kim HJ, Na HS, Park MJ, Chung JM. Abnormalities of sympathetic innervation in the area of an injured peripheral nerve in a rat model of neuropathic pain. *Neurosci Lett* 1993; **162**: 85–88.
9 Devor M. Neuropathic pain and injured nerve: peripheral mechanisms. *Br Med Bull* 1991; **47**: 619–630.
10 Durham PL, Cady R, Cady R. Regulation of calcitonin gene-related peptide secretion from trigeminal nerve cells by botulinum toxin type A: implications for migraine therapy. *Headache* 2004; **44**: 35–42.
11 Coderre TJ, Yashpal K. Intracellular messengers contributing to persistent nociception and hyperalgesia induced by L-glutamate and substance P in the rat formalin pain model. *Eur J Neurosci* 1994; **6**: 1328–1334.
12 McMahon HT, Foran P, Dolly JO, Verhage M, Wiegant VM, Nicholls DG. Tetanus toxin and botulinum toxins type A and B inhibit glutamate, gamma-aminobutyric acid, aspartate, and met-enkephalin release from synaptosomes. Clues to the locus of action. *J Biol Chem* 1992; **267**: 21338–21343.
13 Pretto EA Jr. Reperfusion injury of the liver. *Transplant Proc* 1991; **23**: 1912–1914.
14 Woolfson RG, Millar CG, Neild GH. Ischaemia and reperfusion injury in the kidney: current status and future direction. *Nephrol Dial Transplant* 1994; **9**: 1529–1531.
15 Carroll WR, Esclamado RM. Ischemia/reperfusion injury in microvascular surgery. *Head Neck* 2000; **22**: 700–713.
16 Kasuya A, Sakabe J, Tokura Y. Potential application of in vivo imaging of impaired lymphatic duct to evaluate the severity of pressure ulcer in mouse model. *Sci Rep* 2014; **4**: 4173.
17 Nguyen VA, Eisendle K, Gruber I, Hugl B, Reider D, Reider N. Effect of the dual endothelin receptor antagonist bosentan on Raynaud's phenomenon secondary to systemic sclerosis: a double-blind prospective, randomized, placebo-controlled pilot study. *Rheumatology (Oxford)* 2010; **49**: 583–587.
18 Shenoy PD, Kumar S, Jha LK *et al.* Efficacy of tadalafil in secondary Raynaud's phenomenon resistant to vasodilator therapy: a double-blind randomized cross-over trial. *Rheumatology (Oxford)* 2010; **49**: 2420–2428.
19 Sycha T, Graninger M, Auff E, Schnider P. Botulinum toxin in the treatment of Raynaud's phenomenon: a pilot study. *Eur J Clin Invest* 2004; **34**: 312–313.
20 Van Beek AL, Lim PK, Gear AJ, Pritzker MR. Management of vasospastic disorders with botulinum toxin A. *Plast Reconstr Surg* 2007; **119**: 217–226.
21 Fregene A, Ditmars D, Siddiqui A. Botulinum toxin type A: a treatment option for digital ischemia in patients with Raynaud's phenomenon. *J Hand Surg Am* 2009; **34**: 446–452.
22 Neumeister MW, Chambers CB, Herron MS *et al.* Botox therapy for ischemic digits. *Plast Reconstr Surg* 2009; **124**: 191–201.
23 Neumeister MW. Botulinum toxin type A in the treatment of Raynaud's phenomenon. *J Hand Surg Am* 2010; **35**: 2085–2092.
24 Smith L, Polsky D, Franks AG Jr. Botulinum toxin-A for the treatment of Raynaud syndrome. *Arch Dermatol* 2012; **148**: 426–428.
25 Jenkins SN, Neyman KM, Veledar E, Chen SC. A pilot study evaluating the efficacy of botulinum toxin A in the treatment of Raynaud phenomenon. *J Am Acad Dermatol* 2013; **69**: 834–835.
26 Uppal L, Dhaliwal K, Butler PE. A prospective study of the use of botulinum toxin injections in the treatment of Raynaud's syndrome associated with scleroderma. *J Hand Surg Eur Vol* 2014; **39**: 876–880.
27 Iorio ML, Masden DL, Higgins JP. Botulinum toxin A treatment of Raynaud's phenomenon: a review. *Semin Arthritis Rheum* 2012; **41**: 599–603.
28 Subcommittee for Scleroderma Criteria of the American Rheumatism Association Diagnostic and Therapeutic Criteria Committee. Preliminary criteria for the classification of systemic sclerosis (scleroderma). *Arthritis Rheum* 1980; **23**: 581–590.
29 van den Hoogen F, Khanna D, Fransen J *et al.* 2013 classification criteria for systemic sclerosis: an American College of Rheumatology/European League Against Rheumatism collaborative initiative. *Ann Rheum Dis* 2013; **72**: 1747–1755.
30 LeRoy EC, Black C, Fleischmajer R *et al.* Scleroderma (systemic sclerosis): classification, subsets and pathogenesis. *J Rheumatol* 1988; **15**: 202–205.
31 Sato S, Muroi E, Komura K, Hara T, Ogawa F. The effect of cilostazol on Raynaud's phenomenon in systemic sclerosis patients. *Jpn J Clin Exp Med* 2007; **84**: 88–90 (Japanese).
32 Tomita H, Ogawa F, Kuwatsuka Y, Hara T, Utani A. The effect of preprandial administration of cilostazol on Raynaud's phenomenon in systemic sclerosis patients. *J New Rem & Clin* 2011; **60**: 121–125 (Japanese).
33 Merkel PA, Herlyn K, Martin RW *et al.* Measuring disease activity and functional status in patients with scleroderma and Raynaud's phenomenon. *Arthritis Rheum* 2002; **46**: 2410–2420.
34 Williamson A, Hoggart B. Pain: a review of three commonly used pain rating scales. *J Clin Nurs* 2005; **14**: 798–804.
35 Japan Meteorological Agency: http://www.data.jma.go.jp/obd/stats/etrn/view/monthly_s1.php?prec_no=42&block_no=47624&year=2015&month=&day=&view=p1 (Japanese).
36 Maria G, Brisinda G, Bentivoglio AR, Cassetta E, Gui D, Albanese A. Botulinum toxin injections in the internal anal sphincter for the treatment of chronic anal fissure: long-term results after two different dosage regimens. *Ann Surg* 1998; **228**: 664–669.
37 Schulte-Baukloh H. Botulinum toxin for neurogenic bladder dysfunction. *Urologe A* 2012; **51**: 198–203.
38 Patel S, Martino D. Cervical dystonia: from pathophysiology to pharmacotherapy. *Behav Neurol* 2013; **26**: 275–282.
39 Winner PK, Sadowsky CH, Martinez WC, Zuniga JA, Poulette A. Concurrent onabotulinumtoxinA treatment of cervical dystonia and concomitant migraine. *Headache* 2012; **52**: 1219–1225.
40 Olver J, Esquenazi A, Fung VS, Singer BJ, Ward AB. Cerebral Palsy Institute. Botulinum toxin assessment, intervention and aftercare for lower limb disorders of movement and muscle tone in adults: international consensus statement. *Eur J Neurol* 2010; **17**: 57–73.
41 Kim YS, Roh TS, Lee WJ, Yoo WM, Tark KC. The effect of botulinum toxin A on skin flap survival in rats. *Wound Repair Regen* 2009; **17**: 411–417.
42 Schweizer DF, Schweizer R, Zhang S *et al.* Botulinum toxin A and B raise blood flow and increase survival of critically ischemic skin flaps. *J Surg Res* 2013; **184**: 1205–1213.
43 Kim TK, Oh EJ, Chung JY, Park JW, Cho BC, Chung HY. The effects of botulinum toxin A on the survival of a random cutaneous flap. *J Plast Reconstr Aesthet Surg* 2009; **62**: 906–913.
44 Park TH, Rah DK, Chong Y, Kim JK. The Effects of Botulinum Toxin A on Survival of Rat TRAM Flap With Vertical Midline Scar. *Ann Plast Surg* 2015; **74**: 100–106.
45 Bailey SR, Mitra S, Flavahan S, Flavahan NA. Reactive oxygen species from smooth muscle mitochondria initiate cold-induced

constriction of cutaneous arteries. *Am J Physiol Heart Circ Physiol* 2005; **289**: H243–H250.
46 Flavahan NA. Regulation of vascular reactivity in scleroderma: new insights into Raynaud's phenomenon. *Rheum Dis Clin North Am* 2008; **34**: 81–87.
47 Uchiyama A, Yamada K, Perera B *et al.* Protective effect of botulinum toxin A after cutaneous ischemia-reperfusion injury. *Sci Rep* 2015; **5**: 9072.
48 Meng J, Wang J, Lawrence G, Dolly JO. Synaptobrevin I mediates exocytosis of CGRP from sensory neurons and inhibition by botulinum toxins reflects their anti-nociceptive potential. *J Cell Sci* 2007; **120**: 2864–2874.
49 Carmichael NM, Dostrovsky JO, Charlton MP. Peptide-mediated transdermal delivery of botulinum neurotoxin type A reduces neurogenic inflammation in the skin. *Pain* 2010; **149**: 316–324.

SCIENTIFIC REPORTS

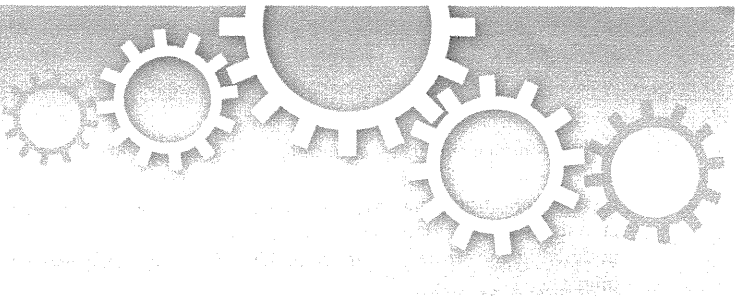

OPEN

SUBJECT AREAS:
SKIN MODELS
ANIMAL DISEASE MODELS

Received
20 October 2014

Accepted
18 February 2015

Published
13 March 2015

Correspondence and requests for materials should be addressed to S.M. (smotegi@gunma-u.ac.jp)

* These authors contributed equally to this work.

Protective effect of botulinum toxin A after cutaneous ischemia-reperfusion injury

Akihiko Uchiyama*, Kazuya Yamada, Buddhini Perera, Sachiko Ogino, Yoko Yokoyama, Yuko Takeuchi, Osamu Ishikawa & Sei-ichiro Motegi*

Department of Dermatology, Gunma University Graduate School of Medicine, Japan.

Botulinum toxin A (BTX-A) blocks the release of acetylcholine vesicles into the synaptic space, and has been clinically used for aesthetic indications, neuromuscular disorders and hyperhidrosis. Several studies have demonstrated that BTX-A enhanced the blood flow and improved ischemia in animal models. Our objective was to assess the effects of BTX-A on cutaneous ischemia-reperfusion (I/R) injuries, mimicking decubitus ulcers. The administration of BTX-A in I/R areas significantly inhibited the formation of decubitus-like ulcer in cutaneous I/R injury mouse model. The number of $CD31^+$ vessels and αSMA^+ pericytes or myofibroblasts in wounds were significantly increased in the I/R mice treated with BTX-A. The hypoxic area and the number of oxidative stress-associated DNA-damaged cells and apoptotic cells in the I/R sites were reduced by BTX-A administration. In an *in vitro* assay, BTX-A significantly prevented the oxidant-induced intracellular accumulation of reactive oxygen species (ROS) in vascular endothelial cells. Furthermore, the administration of BTX-A completely suppressed the ulcer formation in an intermittent short-time cutaneous I/R injury model. These results suggest that BTX-A might have protective effects against ulcer formation after cutaneous I/R injury by enhancing angiogenesis and inhibiting hypoxia-induced cellular damage. Exogenous application of BTX-A might have therapeutic potential for cutaneous I/R injuries.

Ischemia-reperfusion (I/R) injury is characterized by the reperfusion of blood to previously ischemic tissue, which induces excessive cellular injury[1,2]. Reperfusion of blood into a hypoxic tissue can induce a cascade of inflammation, including the infiltration of leukocytes and macrophages and the production of proinflammatory cytokines, resulting in the damages of vascular and lymphatic endothelium, edema, capillary narrowing and the apoptosis and necrosis of tissues[3,4].

Reactive oxygen species (ROS), such as H_2O_2 and NO, also play essential roles in the tissues damage induced by reperfusion[4–9]. I/R injury is associated with vascular infarction or vasospasm in various organs, such as the brain, heart, liver, kidneys and skin. There is also increasing evidence that I/R injury is associated with the pathogenesis of pressure ulcers, also known as decubitus ulcers[10–12]. Raynaud's phenomenon (RP) is commonly observed in response to cold or emotional stress in patients with connective tissue diseases, especially systemic sclerosis. RP is an episodic vasospasm of peripheral blood vessels that results from the dysregulation of vasoconstriction and vasodilatation, suggesting that I/R injury might be involved in the pathogenesis of severe pain and paresthesia of the fingers, as well as the formation of digital ulcers[13,14].

Botulinum toxin (BTX) is a polypeptide produced by the bacterium *Clostridium botulinum*, which contains a protease that plays an active role in inhibiting the acetylcholine release at the neuromuscular junction and the eccrine sweat glands. There are seven (A–G) serotypes of BTX. Type A has been extensively studied and clinically used. Recently, the therapeutic indications of BTX-A have been expanded for axial hyperhidrosis, blepharospasm, facial spasms, cervical dystonia, spasms of the extremities and also for aesthetic indications of facial wrinkles. In addition, there is a broad spectrum of other indications for migraine, achalasia, urinary bladder dysfunction and anal fissures[15–19].

In *in vitro* assays, several reports demonstrated that BTX-A enhanced the blood flow and survival of ischemic skin flaps using animal cutaneous flap models[20–23]. With respect to I/R injury and BTX-A, Küçüker *et al.* showed that BTX-A application suppressed apoptosis and the tissue levels of malonyl dialdehyde (MDA) and nitric oxide end products (NOx) in a rat model of skeletal muscle I/R injury[24]. However, to the best of our knowledge, there have been no studies of the possible effects of BTX-A on cutaneous I/R injuries.

Several case reports have recently demonstrated the beneficial effect of BTX-A in patients with RP, including the enhancement of blood flow and improvement of the digital ulcers, pain and paresthesia of the fingers[25–30]. However, there has been no experimental evidence of the beneficial effects of BTX-A on the I/R injury associated

with RP-induced ulcers using animal models. In this study, we examined the effects of BTX-A on cutaneous I/R injuries in two experimental conditions that mimic decubitus ulcers and RP-induced cutaneous ulcers, respectively, and aimed to clarify the mechanisms underlying the protective effect of BTX-A against cutaneous I/R injury.

Results

Botulinum toxin A protected against ulcer formation in a decubitus ulcer-like I/R injury mouse model. First, to assess the effects of BTX-A on the development of cutaneous pressure ulcers after I/R injury *in vivo*, we compared the wound area in a decubitus ulcer-like I/R injury mouse model treated with or without BTX-A. BTX-A was injected into the dermis at the I/R site 24 hours before the beginning of I/R. The administration of BTX-A significantly inhibited the formation of cutaneous pressure ulcers after I/R injury (Figures 1A, B). At four days after reperfusion, cutaneous ulcers had developed due to I/R injury in the control mice. However, the administration of BTX-A completely protected the mice from ulcer formation in the I/R area (Figures 1A, B). Furthermore, from four to nine days after reperfusion, the wound areas in 1.0 U BTX-A-treated mice were significantly smaller than those in control mice. These results suggest that BTX-A might have the potential to prevent the development of cutaneous pressure ulcers after I/R injury.

Botulinum toxin A protected against the reduction of vascularity induced by cutaneous I/R injury. Kasuya *et al.* recently reported that cutaneous I/R injury induced the suppression of the luminal areas of blood vessels and lymphatic vessels, as well as inducing hypoxia and oxidative stress in the I/R site[4]. In addition, several studies using animal cutaneous flap models demonstrated that BTX-A prevented the collapse of the peripheral vessels in the cutaneous flap and increased the blood flow and survival of the flap[20–23]. Based on these previous studies, we investigated the effects of BTX-A on the vascularity in the I/R area in a cutaneous I/R injury model. At four days after reperfusion, the numbers of $CD31^+$ endothelial cells in I/R areas in BTX-A-treated mice were significantly increased compared to those in control mice (Figure 2A). The numbers of $NG2^+$ pericytes tended to be higher than those in control mice. The numbers of αSMA^+ pericytes or myofibroblasts in I/R areas in BTX-A-treated mice were significantly increased compared to those in control mice (Figure 2B). We confirmed that the stainings using isotype control antibodies were negative. We additionally examined the effect of BTX-A on the vascularity in the I/R area at earlier time point after I/R, such as at 1 hour after reperfusion. The amount of $CD31^+$ endothelial cells, $NG2^+$ pericytes and αSMA^+ pericytes or myofibroblasts in I/R areas in BTX-A-treated mice at 1 hour after reperfusion were significantly increased compared to those in control mice (Supplemental Figure S1A,B). These results suggest that BTX-A might have a preventive effect against the reduction of vascularity by cutaneous I/R injury.

Botulinum toxin A reduced the hypoxic area after cutaneous I/R injury. To examine the influence of BTX-A on the tissue hypoxic area in the cutaneous I/R area after I/R injury in mice, immunofluorescent staining of the hypoxic area using an antibody against pimonidazole, a marker of hypoxia, was performed with skin tissue sections from the I/R area. At one day after reperfusion, the hypoxic area at the I/R site in BTX-A-treated mice was significantly reduced compared to that in control mice (Figure 3). We confirmed that the staining using isotype control antibody was negative. We additionally examined the effect of BTX-A on the hypoxic area in the I/R area at earlier time point after I/R, such as at 1 hour after reperfusion. The amount of hypoxic area in I/R areas in BTX-A-treated mice at 1 hour after reperfusion was significantly reduced compared to that in control mice (Supplemental Figure S1C). These results suggest that BTX-A might have a preventive effect against hypoxia by cutaneous I/R injury in the I/R area.

Botulinum toxin A protected against DNA damage after cutaneous I/R injury. Kasuya *et al.* demonstrated that ROS were produced by I/R injury and created 8-hydroxy-2- deoxyguanosine (8-OHdG), a useful marker of oxidative stress-associated DNA damage, in the DNA of tissue-resident cells[4]. Therefore, we examined the effects of BTX-A on the DNA damage after cutaneous I/R injury by performing immunofluorescent staining of 8-OHdG. At one day after reperfusion, the area with positive staining in the I/R area in BTX-A-treated mice was significantly reduced compared to that in control mice (Figure 4). We confirmed that the staining using isotype control antibody was negative. These results suggest that BTX-A might reduce oxidative stress due to cutaneous I/R injury.

Botulinum toxin A reduced cell apoptosis after cutaneous I/R injury. ROS induced by I/R injury causes apoptosis and subsequent

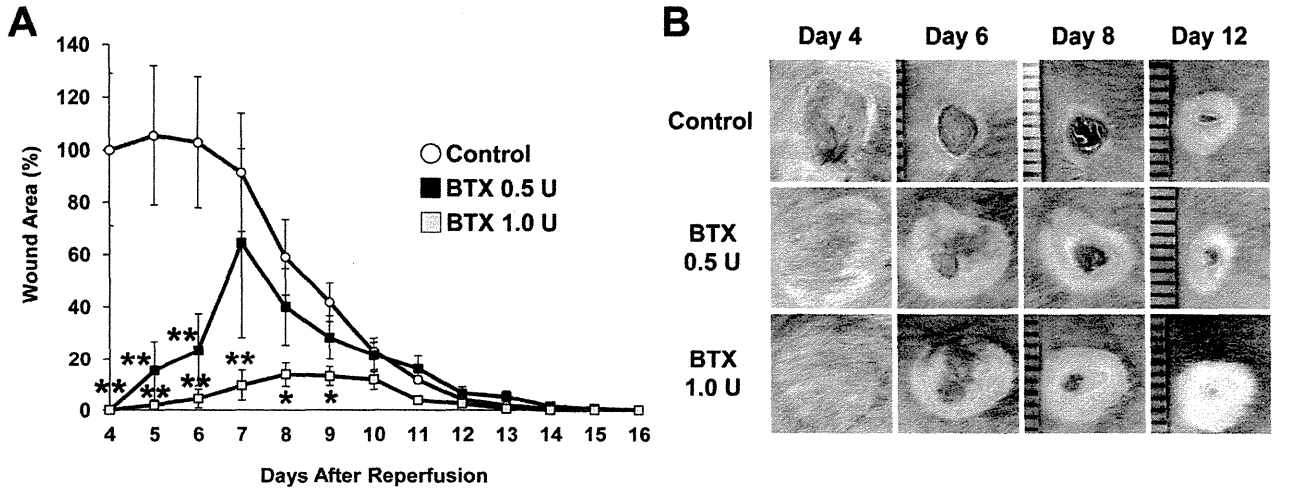

Figure 1 | Botulinum toxin A protected ulcer formation in decubitus ulcer-like I/R injury mice model. (A) Percent wound area at each time point relative to the wound area in control mice at 4 days after reperfusion (n = 7 for each time point and groups). All values represent mean ± SEM. $^{**}P < 0.01$, $^{*}P < 0.05$. (B) Photographs of wound after cutaneous I/R in control or BTX treated mice at 4, 6, 8, and 12 days after reperfusion.